Unitarity and analyticity in reactions with two and three particles in the final state

A. M. Badalyan and Yu. A. Simonov

Institute of Theoretical and Experimental Physics, Moscow
Fiz. Élem. Chastits At. Yadra, **6**, 299–346 (April–June 1975)

The problem is posed of determining the amplitude of scattering and breakup using information that follows from analyticity and unitarity. The three-particle unitarity conditions are written down explicitly, the terms linear (FSI-unitarity) and quadratic in the three-body amplitude being separated. Cases when the three-particle unitarity conditions can be solved explicitly by means of the Hilbert–Schmidt representation are investigated as an illustration. Other published methods using analyticity and unitarity in scattering and breakup reactions are discussed briefly.

PACS numbers: 11.80.

INTRODUCTION

In this review, an attempt is made to generalize the existing results on use of unitarity and analyticity in the theory of nuclear reactions. There is an extensive literature[1,2] for reactions with two particles in the initial and the final state. Attention will therefore be concentrated on methods which can be generalized to reactions with several particles in the final state. Even in this case the literature is very extensive, and we shall focus here mainly on reactions in few-nucleon systems. For such systems, exact calculations have been made for a given nucleon-nucleon interaction, and these calculations can be confronted with approximations in which unitarity and analyticity are taken into account more or less fully. This will show what must be taken into account in approximations and what is less important.

The main question investigated in the review is how one can construct the $2\to 2$ scattering and reaction amplitudes and the $2\to 3$ breakup amplitudes if they are to satisfy the unitarity conditions for two and three particles simultaneously and the analyticity requirements, i.e., have nearest singularities at the necessary places and have there the correct threshold behavior.

The analytic properties of the $2\to 2$ and $2\to 3$ amplitudes can be most readily understood in the language of nonrelativistic Feynman graphs,[3] which correspond to the multiple scattering series in Watson's theory.[4] The analytic properties have been most fully studied for reactions in a system of three particles, in which the graphs correspond to successive iterations of Faddeev's equation.[5]

The most important conclusion drawn from the examination of the nonrelativistic graphs is that the new singularities introduced by the successively more complicated graphs are, first, successively weaker, and, second, successively more distant. This fact is the cornerstone of the theory of direct nuclear reactions,[6] which describes the qualitative behavior of the amplitude by using one or two of the simplest graphs. For example, for the scattering and breakup reaction in the *nd* system the graphs shown in Figs. 1(a) and 1(b) and also in 2(a) and 2(b), respectively, are chosen. It is then found that the qualitative features of these processes are correctly reproduced, but quantitative agreement is lacking at low energies (<40 MeV). At very low energies (~ 1 MeV) the difference between the cross sections reaches two orders of magnitude.[7] For energies $\gtrsim 100$ MeV, these graphs in the *nd* system also give a good quantitative description. This last result is a specific feature of systems with few nucleons—for the reaction on a heavy nucleus allowance for one graph without interaction in the initial and final states does not give the numerically correct result even at arbitrarily high energies.

The physical reason why the description by means of the simplest graphs fails is fairly clear, but different for systems with few or many nucleons. For the former, rescattering on the same nucleons is important at low energies, and the parameter (for isotropic scattering on each nucleon) is fR^{-1}, where f is the scattering amplitude and R the distance between the target nucleons. If the energy is increased, besides the reduction of f there is a further, more important effect—the scattering is through small angles, and the probability of subsequent scattering is strongly reduced. These arguments are inapplicable to heavier nuclei, for which the particle encounters many other centers even in the case of strictly forward scattering. Therefore, in such nuclei (roughly, beginning with carbon) at low energies rescattering on the same nucleon is important as well as scattering on all the remaining nucleons encountered in the path of the scattered particle. At high energies (of the order of several hundred MeV), only the second effect is important, as is allowed for in Glauber's theory.

A reaction amplitude satisfying all physical requirements can be constructed in three ways:

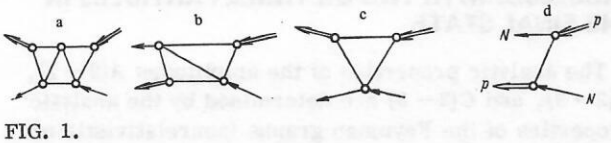

FIG. 1.

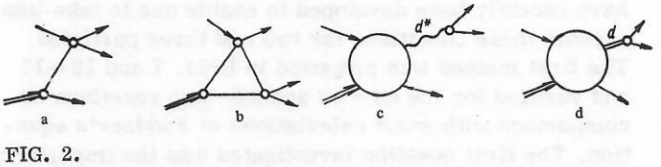

FIG. 2.

1) by the phenomenological approach and the construction of an optical potential for the particle-target interaction, its parameters being either freely disposable or determined by theoretical data;

2) by a dynamical approach. Here, one proceeds from a given elementary interaction (nucleon-nucleon) and solves the Schrödinger or an equivalent equation (Faddeev, Faddeev-Yakubovskiĭ, and so forth) numerically;

3) the S-matrix approach.[8] In complete analogy with the theory of elementary particles, one assumes that knowledge of the singularities of the amplitude and unitarity enable one to construct the amplitude uniquely.

It is the S-matrix approach we shall investigate here. In addition to the graphical method, one uses unitarity, by means of which rescattering of the particle on each of the target particles can be taken into account. Unitarity is exploited in quite different ways in the following situations: a) elastic scattering $2 \to 2$; b) inelastic scattering $2 \to 2'$; c) the reaction $2 \to n$, $n \geq 3$.

In case a) unitarity can be taken into account very simply even if open inelastic channels are present: It is easy to write down the general form of an amplitude that satisfies two-particle unitarity either for the partial waves, or in the impact-parameter representation, or in the form of the optical theorem for the forward dispersion relations, etc. Case b) is the many-channel two-particle problem, which generalizes the formal solution for case a) through the introduction of a matrix of amplitudes, as is done in the R-matrix theory of nuclear reactions.[1]

Case b) exhibits some specific features if one uses the graphical approach or the approximation of a single inelastic interaction.[4] Here, if the inelastic interaction is much less probable than the elastic (for example, as in the diffraction excitation of nuclear levels), it is sufficient to unitarize only the initial and final interactions, regarding them as elastic interactions. This can be done in the framework of either the DWBA method[9] or S-matrix theory.[10] If it is assumed that the $a+A$ and $b+B$ elastic scattering amplitudes for the reaction $a+A \to b+B$ (or the optical potential corresponding to these channels) are known, the general form of the amplitude of this inelastic reaction that is unitary with respect to the initial and (or) the final interaction can be written down.[11]

Finally, the reactions $2 \to n$, $n \geq 3$, of case c) present the greatest difficulties. Here, we restrict ourselves to $n=3$, having in mind the breakup reactions $nd \to nnp$ as the first concrete application. But the problem will be formulated generally, so that the results can be readily transferred to any reactions of the form $2 \to 3$. The main difficulty is to satisfy the three- and two-particle unitarity conditions simultaneously. Different methods have recently been developed to enable one to take into account these conditions for two and three particles. The first method was proposed in Refs. 7 and 12—15 and verified for the $nd \to nd$ and $nd \to nnp$ reactions by comparison with exact calculations of Faddeev's equation. The first question investigated was the importance of allowing for three-particle intermediate states in the unitarity conditions for both reactions. The answer was somewhat unexpected: Elastic unitarization of the two simplest graphs in Figs. 1(a) and 1(b) and 2(a) and 2(b) for these reactions, i.e., allowance for only intermediate nd states, is already adequate to remove most of the strong discrepancy between the exact result and the graph contribution discussed above.[7,12] This means that for the inelastic $nd \to nnp$ reaction it is important to take into account the interaction in the initial state and in the first approximation ignore rescattering in the state of the three final unbound particles. Finally, the method forsees exact allowance for the unitarity conditions, though in a very cumbersome manner.[13,15]

Another way of constructing unitary and analytic amplitudes was proposed in Refs. 16 and 17 on the basis of the Hilbert-Schmidt representation. Its advantage is that the $2 \to 2$ and $2 \to 3$ amplitudes are represented by series of terms each of which corresponds to a real or virtual pole or a resonance in the total energy, and the residues separate with respect to the initial and final momenta. Then in the construction of the unitary amplitude the denominator is expressed in terms of residues (vertex functions), as in the UPA approximation for two particles.[18] One may say that if this method is restricted to one term it is the UPA approximation for three particles; but if all the terms of the Hilbert-Schmidt representation are taken, the exact result is obtained.

Here we shall investigate the convergence of the Hilbert-Schmidt series and illustrate it by numerical examples (the convergence is very rapid). The method is also very natural for the description of resonance states, in particular, three-particle resonance states.

Whatever approach is used to construct the unitary three-particle amplitude, one has to take into account the final-state interaction of a pair of particles (the FSI term in the three-particle unitarity condition). This problem reduces to the solution of a homogeneous integral equation, which can be solved exactly in limiting cases. This question is also analyzed in the review. Here, we shall not consider the generalization of the method to four-particle states, for which it has recently been used with success.[19] Nor (for the same reason) shall we consider here the relativistic generalization of the Hilbert-Schmidt representation.

To summarize, let us point out that the use of three-particle unitarity conditions in the framework of analyticity and unitarity has only just begun. But it already enables one to describe three-particle processes accurately and has great promise for the detailed development of a quantitative theory of nuclear reactions with three or more particles in the final state and also for the theory of three-particle resonances and the amplitudes of three- and many-particle decays.

1. ANALYTIC PROPERTIES OF AMPLITUDES OF PROCESSES WITH TWO OR THREE PARTICLES IN THE FINAL STATE

The analytic properties of the amplitudes $A(2 \to 2)$, $B(2 \to 3)$, and $C(3 \to 3)$ are determined by the analytic properties of the Feynman graphs (nonrelativistic or

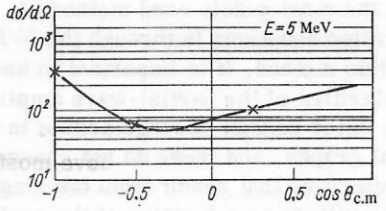

FIG. 3.

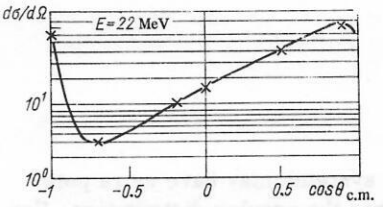

FIG. 4.

relativistic) corresponding to the given processes, i.e., by the singularities of the graphs with respect to all the independent kinematic variables. In addition, there may be singularities of the complete sum of graphs: poles with respect to the total energy corresponding to bound states and resonances. We assume (though no one has yet proved this) that these singularities exhaust all possibilities.

One then obtains a simple qualitative picture which explains the form of the experimental angular and energy distributions. This picture is the basis of the graphical theory of direct nuclear reactions.[6,20] The connection between the singularities of the simplest graphs and the form of the angular and energy distributions was followed in its clearest quantitative form for *nd* scattering and breakup; it is these processes that we shall mainly discuss.

For *nd* scattering, $A(2\to 2)$ depends on two variables: the energy E and x, the cosine of the scattering angle. As a function of the energy (for fixed x), A in the physical region has only a threshold singularity, which is associated with the opening of the $2\to 3$ channel at $E_{c.m}=\epsilon$; this has the form $(E-\epsilon)^2\ln(E-\epsilon)$ and therefore is hardly manifested in the energy dependence of the total and differential cross sections.[21] All the graphs of Fig. 1 except Fig. 1(a) have this singularity.

The angular dependence is different: the nearest singularity in x (pole) derives from Fig. 1(a) and is at

$$x=x_0\equiv -5/4-(3/4)(\epsilon/E), \tag{1}$$

i.e., fairly near the physical region. This shows that the angular distribution must have a backward peak, its height increasing with the energy. Both conclusions are confirmed experimentally (Figs. 3 and 4; data taken from the review Ref. 21).

In contrast to Fig. 1(a), Fig. 1(b) has a singularity in x nearer to the other edge of the physical region:

$$x=x_1=2x_0^2-1\equiv 17/8+(15/4)(\epsilon/E)+(9/8)(\epsilon^2/E^2). \tag{2}$$

This singularity must lead to a forward peak in the angular distribution. In addition, since the singularity (2) is further from the physical region than (1), the forward peak must be flatter. And, as can be seen from Figs. 3 and 4 and also many other data,[21] the forward peak and the backward peak are the most important characteristics of the angular distributions in a wide range of energies—from tenths of an MeV to several hundred MeV.

Knowing the singularities of Figs. 1(a) and 1(b), one can find those of all the remaining more complicated graphs by the so-called block method of investigating singularities proposed in Ref. 22. It can be shown that all graphs with an even number of vertices have singularities to the left of $x=-1$; graphs with an odd number of vertices (like Fig. 1(b)), to the right of $x=1$. In addition, the singularities move further away from the physical region with increasing of order of the graph, becoming less strong. This last agrees with the more general assertion that when the order of a graph is increased a singularity with respect to all variables becomes less well expressed.[5]

Note, and this will be proved later, that a backward peak necessarily entails a forward peak by unitarity. Another way of understanding this is to regard the unitarity conditions as an iteration mechanism which reproduces Fig. 1(b) on the substitution of Fig. 1(a) as a first approximation, and so forth. All this remains true for scattering on objects more complicated than the deuteron: The position of the singularities (1) and (2) is shifted, but the general picture remains, a poletype graph leading to a backward peak and a triangular graph to a forward peak.

We now turn to breakup processes $(2\to 3)$. These reactions have been investigated on the basis of the angular distributions in two situations: when two of the three final particles are in the region of strong interaction because of the Migdal-Watson effect (the interaction peak in the final state is an FSI peak) and when integration is performed over the complete energy spectrum. In the first case, the situation is like that considered already for elastic scattering since the two particles in the FSI peak can be regarded as one (deuteron or singlet deuteron d^* for the *np* system and d^* for the *pp* system). Figures 2(a) and 2(b) indicate the presence of singularities near the forward and backward directions, and these are manifested experimentally in the breakup reaction $d(np)2n$ at 14, 46, and 50 MeV (see Fig. 10 of Ref. 23). The peaks are smoothed as a result of integration over the whole spectrum of the final particles since the contribution of Figs. 2(a) and 2(b) is not distinguished from other contributions and, in addition, the position of the singularities in these graphs moves with varying energy of the final particle pair.

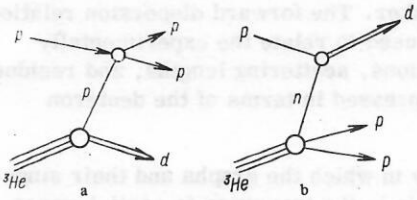

FIG. 5.

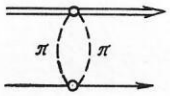

FIG. 6.

More complicated systems may have more pole graphs, which changes the angular distribution. For example, in the reaction ^{3}He$(p,d)2p$ the two pole diagrams Figs. 5(a) and 5(b) are possible, and they lead to singularities in the cosine of the angle between the initial proton and the final deuteron in different regions: Fig. 5(a) gives a singularity near $x=-1$, whereas Fig. 5(b) gives a pole singularity near $x=1$. The latter is manifested experimentally as a sharp peak (see Fig. 6 of Ref. 23).

The amplitude $B(2\to 3)$ has altogether five kinematic variables. In particular, one can choose the total energy, the energy of a pair of the three final particles (there are two such variables) and two variables of the type of a momentum transfer or the corresponding scattering angle between the initial particle and one final particle. We have already discussed the most intensively studied distributions, namely, those when a pair of the final particles is in an FSI peak, i.e., when the analytic and kinematic properties of the $2\to 3$ reaction hardly differ from the $2\to 2$ reactions. The singularities in the energy dependences are due to the graphs of Figs. 2(a), 2(c), and 2(d) (Fig. 2(b) is a special case of Figs. 2(c) and 2(d)).

The first of these diagrams leads to a peak at low energy of the final spectator particle (a quasifree-scattering peak, or QFS peak); the other two, to an FSI peak. The majority of experiments have been and are aimed at investigating these regions. Unfortunately, singularities with respect to other variables and also more complicated singularities connecting several variables and corresponding to more complicated graphs have hardly been studied at all in nuclear reaction experiments (see, for example, the review Ref. 20).

On the theoretical front, the singularities of the simplest (and therefore most singular) graphs are usually used at two levels. First, important information can be extracted from the forward dispersion relations since the imaginary part on the right-hand cut in this case can be expressed in terms of the total cross section by means of the optical theorem. The exchange diagram (see Fig. 1(a)) is distinguished by its having a pole in the energy for the forward direction at the point

$$E_{c.m}=-\epsilon/3, \tag{3}$$

where $E_{c.m}=(3/4)(p^2/m)$, or one can also use the variable $z=E_{c.m}-\epsilon$. Other singularities, for example, those corresponding to Fig. 1(c), are much further away and are weaker. The forward dispersion relation can therefore be used to relate the experimentally known cross sections, scattering lengths, and residue at the pole (3) expressed in terms of the deuteron vertices.

The second way in which the graphs and their singularities are used is in the transition to partial waves. Since the unitarity relation in such a case is quadratic and is diagonalized, the most widely used method of solution of the dispersion equations is through the N/D approximation.[24] In this method, it is important to know all the nearest singularities of the partial-wave amplitudes. As usual, the latter consist of singularities in the energy of the original graphs, and these do not change at all, and also of singularities that result from the singularities of the total amplitude as a function of the angle (transition of singularities in the u and t channels to singularities of the partial-wave amplitudes in the S channel). Concretely, for nd scattering we obtain a left-hand cut with branch points corresponding to different graphs. For example, the graph (see Fig. 1(a)) gives a logarithmic branch point at $z=z_1=-4\epsilon/3$, where $z=E_{c.m}-\epsilon$, and ϵ is the deuteron binding energy. The next most complicated graph, Fig. 1(b), leads to a branch point at $z_2=-4\epsilon$.

Besides the singularities in the series of multiple scattering graphs (see Fig. 1), one must also consider graphs including the exchange of pions (Figs. 6 and 7). The first of them leads to a singularity of the type $(z-z_3)^{3/2}$, where $z_3=-3m_\pi^2/4M-\epsilon\approx-8.1\epsilon$. The graph in Fig. 7 has an anomalous and a normal singularity.

The first is at $z_4=-m_\pi^2/3M-(2m_\pi/3)\sqrt{\epsilon/M}-4\epsilon/3\approx-7.2\epsilon$ and has the form $(z-z_4)\ln(z-z_4)$, while the second is much further away (at $z=z_5=-4\epsilon/3-m_\pi/3-m_\pi^2/6M\approx-23\epsilon$). We see that the most important singularities—both as regards their proximity and strength—are those of the simplest graph (Fig. 1(a)); this is the justification for using it as the main dynamical mechanism in the most varied approaches.

The above correspondence between the angular distribution and the singularities of the simplest graphs is very approximate. If these graphs are used to describe quantitatively scattering and breakup, they lead to a strong discrepancy with the experiments (except at high energies, $E\gtrsim 100$ MeV). The reason for the discrepancy becomes clearer if one attempts to substitute the first graphs into the unitarity conditions. The unitarity conditions are strongly violated, their left- and right-hand sides can differ by an order of magnitude at low energies. It is therefore desirable, on the basis of the simplest graphs, to construct an approximate amplitude that does satisfy the conditions and must then lead to better agreement with the experiments. Such approaches are discussed in Sec. 3.

2. UNITARITY RELATIONS

In the introduction we have already pointed out how important it is at low energies to take into account exactly or approximately the three-particle unitarity conditions, and we discussed different schemes devoted to their investigation. Here we dwell on the derivation of the unitarity conditions for three-particle amplitudes describing three identical particles. In this case, there

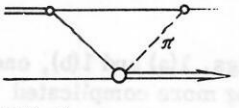

FIG. 7.

is no need to consider detailed amplitudes[5] of the type $M_{\alpha\beta}$, for which the unitarity conditions were investigated in Ref. 13; instead we can introduce a single function w, which determines[25] all the physical amplitudes of scattering and breakup and $3 \to 3$. It is important that these conditions will not be written down in operator form but as equations, so that the unitarity conditions can be readily written down for the partial-wave amplitudes.

It is well known that the three-particle T matrix in the general case is determined by nine functions $M_{\alpha\beta}$ [5]:

$$T(z) = \sum_{\alpha,\beta} M_{\alpha\beta}(z), \tag{4}$$

where α and β are the ingoing and outgoing channels; they are specified by the labeling of the particles; the $M_{\alpha\beta}$ contain unconnected graphs which do not occur in the cross sections of physical processes and must be subtracted:

$$M_{\alpha\beta} = W_{\alpha\beta} + \delta_{\alpha\beta} T_\alpha(z). \tag{5}$$

For identical particles, both with and without spin, the physical amplitudes can be expressed in terms of two functions:

$$\left.\begin{aligned} W^{(1)}(z) &\equiv W_{\alpha\alpha}(z); \\ W^{(2)}(z) &\equiv W_{\alpha\beta}(z), \quad \alpha \neq \beta. \end{aligned}\right\} \tag{6}$$

We now note that for identical particles the experimentally observed amplitude must be averaged over all possible initial and final labelings of the particles. We then find[25] that the cross sections of the processes are determined by the symmetrized amplitude

$$w = W^{(1)} + 2W^{(2)}. \tag{7}$$

From the equation for $W_{\alpha\beta}$ (see Ref. 5) one can obtain an equation for $w(\mathbf{kp}; \mathbf{k'p'}; z)$. Here, $\mathbf{k}, \mathbf{p}$ and $\mathbf{k'}, \mathbf{p'}$ are the momenta of the pair of interacting particles and the third particle in the initial and final states, respectively, and $\mathbf{k}$ and $\mathbf{p}$ are related to the momenta of the individual particles in the usual manner.[5]

In all that follows we shall assume for simplicity that the relative angular momentum l of the pair of interacting particles is zero at the beginning and the end, the third particle having arbitrary angular momentum L. The restriction $l=0$ is not stringent since it is known that in the solution of Faddeev's equation even with realistic potentials it is usually sufficient to take only the two partial waves with $l=0$ and 2. It is easy to show[25] that $w(k\mathbf{p}, k'\mathbf{p}, z)$ satisfies

$$\begin{aligned} &w(k\mathbf{p}, k'\mathbf{p}'; z) \\ &= -\frac{2mt(k, |\mathbf{p}/2+\mathbf{p}'|; z-3p^2/4m)\, t(|\mathbf{p}+\mathbf{p}'/2|, k'; z-3p'^2/4m)}{p^2+\mathbf{pp}'+p'^2-mz} \\ &-2m\int d\mathbf{p}_1 \frac{t(k, |\mathbf{p}/2+\mathbf{p}_1|; z-3p^2/4m)\, w(|\mathbf{p}+\mathbf{p}_1/2|, \mathbf{p}_1; k'\mathbf{p}'; z)}{p^2+\mathbf{pp}_1+p_1^2-mz}. \end{aligned} \tag{8}$$

Here m is the mass of the particle and $t(k, k', z)$ is the two-particle t matrix.

From this we directly obtain the unitarity conditions for w, which we write on the energy shell, i.e., when $z = k^2/m + 3p^2/4m = k'^2/m + 3p'^2/4m$. The discontinuity of w is conveniently represented as a sum of five terms, each of them having a simple physical meaning which will be discussed below:

$$\begin{aligned} \Delta w &= w(z_1) - w(z_2) = \Delta_1 + \Delta_2 + \Delta_3 + \Delta_4 + \Delta_5; \\ z_1 &= E + i\delta; \quad z_2 = E - i\delta, \end{aligned} \tag{9}$$

where

$$\Delta_1 = -2\pi i m t(k, |\mathbf{p}/2+\mathbf{p}'|; z_1 - 3p^2/4m) \times t(|\mathbf{p}+\mathbf{p}'/2|, k'; z_2 - 3p'^2/4m)\, \delta(p^2+\mathbf{pp}'+p'^2-mz); \tag{10}$$

$$\left.\begin{aligned} \Delta_2 &= \Delta_{2d} + \Delta_{2n}; \\ \Delta_{2d} &= -2\pi i m \int d\mathbf{q}\, t(k, q; z_1 - 3p^2/4m) \times w(q\mathbf{p}, k'\mathbf{p}'; z_2)\, \delta(q^2+3p^2/4-mz); \\ \Delta_{2n} &= -4\pi i m \int d\mathbf{p}_1 t(k, |\mathbf{p}/2+\mathbf{p}_1|, z_1 - 3p^2/4m) \times w(|\mathbf{p}+\mathbf{p}_1/2|, \mathbf{p}_1, k', \mathbf{p}'; z_2)\, \delta(p^2+\mathbf{pp}_1+p_1^2-mz); \end{aligned}\right\} \tag{11}$$

$$\left.\begin{aligned} \Delta_3 &= \Delta_{3d} + \Delta_{3n}, \\ \Delta_{3d} &= -2\pi i m \int d\mathbf{q} w(k\mathbf{p}, q\mathbf{p}_1; z_1) \times t(q, k'; z_2 - 3p'^2/4m)\, \delta(q^2+3p'^2/4-mz); \\ \Delta_{3n} &= -4\pi i m \int d\mathbf{p}_1 w(k\mathbf{p}, |\mathbf{p}_1/2+\mathbf{p}'|, \mathbf{p}_1; z_1) \times t(|\mathbf{p}'/2+\mathbf{p}_1|, k'; z_2 - 3p'^2/4m)\, \delta(p'^2+\mathbf{p}'\mathbf{p}_1+p_1^2-mz); \end{aligned}\right\} \tag{12}$$

$$\left.\begin{aligned} \Delta_4 &= \Delta_{4d} + \Delta_{4n}; \\ \Delta_{4d} &= -2\pi i m \int\int d\mathbf{q}\, d\mathbf{p}_1 w(k\mathbf{p}, q\mathbf{p}_1; z_1)\, w(q\mathbf{p}_1, k'\mathbf{p}'; z_2) \times \delta(q^2+3p_1^2/4-mz); \\ \Delta_{4n} &= -4\pi i m \int\int d\mathbf{p}_1\, d\mathbf{p}_2 w(k\mathbf{p}; |\mathbf{p}_2+\mathbf{p}_1/2|, \mathbf{p}_1; z_1) \times w(|\mathbf{p}_1+\mathbf{p}_2/2|, \mathbf{p}_2; k'\mathbf{p}'; z_2)\, \delta(p_1^2+\mathbf{p}_1\mathbf{p}_2+p_2^2-mz); \end{aligned}\right\} \tag{13}$$

$$\Delta_5 = -2\pi i m \int d\mathbf{p}_1 \tilde{B}(k\mathbf{p}, \mathbf{p}_1; z_1)\, B(\mathbf{p}_1, k'\mathbf{p}'; z_2)\, \delta(3p_1^2/4 - \alpha^2 - mz); \tag{14}$$

α is the deuteron wave vector: $\alpha^2 = m\epsilon$; ϵ is the deuteron binding energy. Equation (14) contains the breakup amplitude B and the amplitude $\tilde{B}$ of the process $3 \to 2$, which are related to w by (16) and (17).

The unitarity relations (10)—(14) can be given a simple graphical representation, which is essentially similar to that in Ref. 13. The graphs corresponding to all the discontinuities, $\Delta_1 - \Delta_5$, are shown in Figs. 8—12. The crossed lines in the graphs mean that the propagators must be replaced by corresponding δ functions. It is easy to see that Δ_1 is the inhomogeneous term of the unitarity condition. We shall say that the associated singularity is dynamical. The singularities Δ_{2d}, Δ_{2n}, and Δ_{3d}, Δ_{3n} derive from the interaction in the initial and final states, and, as can be seen from (11) and (12), all these terms are linear in w. We shall call them singularities of FSI type. Finally, the last three terms, Δ_{4d}, Δ_{4n}, and Δ_5, are quadratic in w and give the ordinary unitary singularities in z beginning with $z=0$ for Δ_{4d} and Δ_{4n} (three-particle unitary cut) and with $z=-\epsilon$ for Δ_5, which corresponds to the two-particle unitary cut.

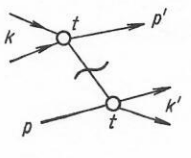

FIG. 8.

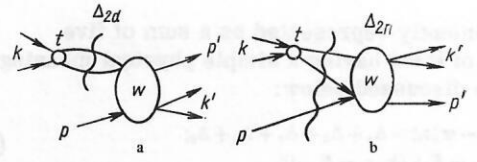

FIG. 9.

Clearly, the physical amplitude of the $3 \to 3$ process is determined by the function $w(k\mathbf{p}, k'\mathbf{p}'; z)$ itself, while the amplitudes of elastic scattering $A(\mathbf{p},\mathbf{p}'; z)$ and breakup $B(\mathbf{p}; k'\mathbf{p}'; z)$ are determined by the residues at the corresponding deuteron poles:

$$w(k\mathbf{p}, k'\mathbf{p}'; z) = \frac{\varphi(k)\, A(\mathbf{p}, \mathbf{p}'; z)\, \overline{\varphi}(k')}{(z+\alpha^2/m-3p^2/4m)(z+\alpha^2/m-3p'^2/4m)} + \frac{\widetilde{b}(k\mathbf{p}, \mathbf{p}'; z)\, \overline{\varphi}(k')}{z+\alpha^2/m-3p^2/4m} + \frac{\varphi(k)\, b(\mathbf{p}, k'\mathbf{p}'; z)}{z+\alpha^2/m-3p^2/4m} + c(k\mathbf{p}, k'\mathbf{p}'; z). \tag{15}$$

Here, $\varphi(k)$ is the deuteron wave function, and $c(k\mathbf{p}, k'\mathbf{p}'; z)$ does not contain pole terms. It is obvious from (15) that the breakup amplitude and similarly the $3 \to 2$ amplitude $\widetilde{B}(k\mathbf{p}, \mathbf{p}'; z)$ are given by

$$B(\mathbf{p}, k'\mathbf{p}'; z) = \frac{A(\mathbf{p}, \mathbf{p}'; z)\, \overline{\varphi}(k')}{z+\alpha^2/m-3p'^2/4m} + b(\mathbf{p}, k'\mathbf{p}'; z); \tag{16}$$

$$\widetilde{B}(k\mathbf{p}, \mathbf{p}'; z) = \frac{\varphi(k)\, A(\mathbf{p}, \mathbf{p}'; z)}{z+\alpha^2/m-3p^2/4m} + \widetilde{b}(k\mathbf{p}, \mathbf{p}'; z). \tag{17}$$

For the elastic scattering amplitude, we have $z = -\alpha^2/m + 3p^2/4m = -\alpha^2/m + 3p'^2/4m$ by the law of conservation of energy, so that the discontinuities Δ_1, Δ_2, and Δ_3 in (10)–(12) are zero. In the breakup process $z = -\alpha^2/m + 3p^2/4m = k^{2\prime}/m + 3p^{2\prime}/4m$, and, as before, $\Delta_1 = \Delta_2 = 0$, but $\Delta_3 \neq 0$. For such physical values of z, we obtain the following unitarity conditions for the amplitudes A and B:

$$\begin{aligned}\Delta A = -2\pi i m \Big\{ &\int d\mathbf{p}_1 A(\mathbf{p}, \mathbf{p}_1; z_1)\, A(\mathbf{p}_1, \mathbf{p}'; z_2)\, \delta(3p_1^2/4 - \alpha^2 - mz) \\ &+ \int\int d\mathbf{q}\, d\mathbf{p}_1 B(\mathbf{p}, q\mathbf{p}_1; z_1)\, \widetilde{B}(q\mathbf{p}_1, \mathbf{p}'; z_2)\, \delta(q^2 + 3p_1^2/4 - mz) \\ &+ 2\int\int d\mathbf{p}_1\, d\mathbf{p}_2 B(\mathbf{p}; |\mathbf{p}_2 + \mathbf{p}_1/2|, \mathbf{p}_1; z_1) \times \\ &\times \widetilde{B}(|\mathbf{p}_1 + \mathbf{p}_2/2|, \mathbf{p}_2; \mathbf{p}'; z_2)\, \delta(p_1^2 + \mathbf{p}_1\mathbf{p}_2 + p_2^2 - mz) \Big\};\end{aligned} \tag{18}$$

$$\begin{aligned}\Delta B = -2\pi i m \Big\{ &\int d\mathbf{q} B(\mathbf{p}, q\mathbf{p}'; z_1)\, t(q, k'; z_2 - 3p'^2/4m) \\ &\times \delta(q^2 + 3p'^2/4 - mz) + 2\int d\mathbf{p}_1 B(\mathbf{p}; |\mathbf{p}_1/2 + \mathbf{p}'|, \mathbf{p}_1; z_1) \\ &\times t(|\mathbf{p}'/2 + \mathbf{p}_1|, k'; z_2 - 3p'^2/4m)\, \delta(p'^2 + \mathbf{p}'\mathbf{p}_1 + p_1^2 - mz)\end{aligned}$$

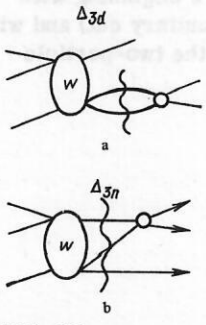

FIG. 10.

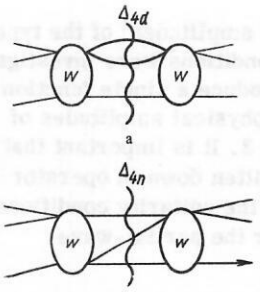

FIG. 11.

$$\begin{aligned}&+ \int\int d\mathbf{q}\, d\mathbf{p}_1 B(\mathbf{p}, q\mathbf{p}_1; z_1)\, w(q\mathbf{p}_1, k'\mathbf{p}'; z_2)\, \delta(q^2 + 3p_1^2/4 - mz) \\ &+ 2\int\int d\mathbf{p}_1\, d\mathbf{p}_2 B(\mathbf{p}, |\mathbf{p}_2 + \mathbf{p}_1/2|, \mathbf{p}_1, z_1)\, w(|\mathbf{p}_1 + \mathbf{p}_2/2|, \mathbf{p}_2; k'\mathbf{p}'; z_2) \\ &\times \delta(p_1^2 + \mathbf{p}_1\mathbf{p}_2 + p_2^2 - mz) + \\ &+ \int d\mathbf{p}_1 A(\mathbf{p}, \mathbf{p}_1; z_1)\, B(\mathbf{p}_1, k'\mathbf{p}'; z_2)\, \delta(3p_1^2/4 - \alpha^2 - mz) \Big\}.\end{aligned} \tag{19}$$

The scattering and breakup amplitude was defined above without reference to the labeling of identical particles. It is obvious that for the scattering process (*nd* process) the labeling can be fixed, and is therefore unimportant. But the amplitudes of breakup B and of the $3 \to 3$ process are by their very construction related to a definite labeling of the particles. Therefore, the experimentally observed breakup amplitude can be obtained from (16) by symmetrization with respect to all possible final states (for spinless particles). Thus, if experimentally in the $nd \to nnp$ process we measure the direction and energy of the proton, i.e., its momentum $\mathbf{p}_f$, and the two other particles have relative momentum $\mathbf{k}_f$, the symmetrized amplitude is[17]

$$\begin{aligned}B^s(\mathbf{p}, \mathbf{k}_f\mathbf{p}_f; z) = \{&B(\mathbf{p}; \mathbf{k}_f\mathbf{p}_f; z) \\ &+ B(\mathbf{p}; -\mathbf{k}_f/2 - 3\mathbf{p}_f/4; -\mathbf{p}_f/2 + \mathbf{k}_f; z) \\ &+ B(\mathbf{p}; -\mathbf{k}_f/2 + 3\mathbf{p}_f/4; -\mathbf{p}_f/2 - \mathbf{k}_f; z)\}/3.\end{aligned} \tag{20}$$

The unitarity condition for the scattering amplitude can be written in a more compact form by means of this symmetrized amplitude. It is also convenient to replace A by the ordinary scattering amplitude f, which differs from A by a normalizing factor:

$$f(\mathbf{p}, \mathbf{p}'; z) = -8\pi^2 m A(\mathbf{p}, \mathbf{p}'; z)/3, \tag{21}$$

and also

$$g^s(\mathbf{p}, \mathbf{k}_f\mathbf{p}_f; z) = -8\pi^2 m B^s(\mathbf{p}, \mathbf{k}_f\mathbf{p}_f; z)/3. \tag{22}$$

Then (18) is replaced by

$$\begin{aligned}\operatorname{Im} f(\mathbf{p}, \mathbf{p}'; z) = \Big\{ &\int d\mathbf{p}_1 f(\mathbf{p}, \mathbf{p}_1; z)\, f^*(\mathbf{p}_1, \mathbf{p}'; z)\, \delta(p_1^2 - 4\alpha^2/3 - 4mz/3) \\ &+ 3\int d\mathbf{k}_1\, d\mathbf{p}_1 g^s(\mathbf{p}, \mathbf{k}_1\mathbf{p}_1; z)\, g^{s*}(\mathbf{p}'; \mathbf{k}_1\mathbf{p}_1)\, \delta(p_1^2 + 4k^2/3 - 4mz/3) \Big\}/2\pi.\end{aligned} \tag{23}$$

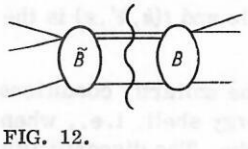

FIG. 12.

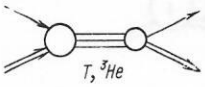

FIG. 13.

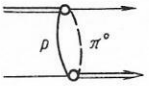

FIG. 14.

On the transition in (18) from the $3 \to 2$ amplitude $\tilde{B}$ to the amplitude g^{s*} we used the identity satisfied by the function $w(k\mathbf{p},\ k'\mathbf{p}';\ z)$:

$$w(k\mathbf{p};\ k'\mathbf{p}';\ z^*) = w^*(k'\mathbf{p}';\ k\mathbf{p};\ z). \tag{24}$$

From (23) and the optical theorem, $\mathrm{Im} f(\theta=0) = p\sigma_{\mathrm{tot}}/4\pi$, we readily find expressions for the differential and total cross sections of elastic and inelastic scattering. Thus

$$d\sigma_{el}/d\Omega = |f(\mathbf{p},\ \mathbf{p}';\ z)|^2 \tag{25}$$

and

$$d\sigma_{\mathrm{inel}}\, d\mathbf{p}_f = 9k_f\, 4p \int_{\Omega} |g^s(\mathbf{p},\ \mathbf{k}_f\mathbf{p}_f;\ z)|^2\, d\Omega_k. \tag{26}$$

It is assumed in (26) that in the breakup process a particle in the direction $\mathbf{p}_f$ and with energy $\epsilon_f = p_f^2/2m$ is detected. The limits of integration in (26) are determined by the kinematics of the problem. All the momenta are here referred to the center of mass system.

Introducing the partial-wave amplitudes f_L and g_L, we also find the total partial-wave cross sections:

$$\sigma_{\mathrm{inel}}^L = \frac{36\pi^2}{p}(2L+1)\int\int d\Omega_{\varkappa}\, dp_1 \varkappa_1 p_1^2 \theta(mz - 3p^2/4)\, |g_L^s(p,\ \varkappa_1\mathbf{p}_1;\ z)|^2; \tag{27}$$

$$\sigma_{\mathrm{el}}^L = 4\pi(2L+1)\, |f_L(p,\ z)|^2. \tag{28}$$

Here $\varkappa_1^2 = mz - 3p_1^2/4$ and the amplitude g_L^S in reality depends on the angle between $\varkappa_1$ and $\mathbf{p}_1$.

3. METHODS USING UNITARITY AND ANALYTICITY

Unitarity and analyticity have been used most widely in calculations of scattering and $2 \to 2$ reactions. In this case, the most natural approach is the method of dispersion relations, which has been used in three different modifications: 1) at a given angle; 2) with respect to the momentum transfer or the cosine of the angle; 3) for partial waves. All methods are based on analyticity as a means of relating the amplitude at a given physical point to its values (or rather to the values of its imaginary part) in other regions. The contribution of these other regions enters in the form of an integral with respect to positive energies, and these can be expressed by unitarity in terms of the cross section or the square of the amplitude, and in the form of an integral (or pole term) over the unphysical region of negative energies. The last term depends on the mechanism of the process. For example, for potential scattering it is determined by the form of the potential. Therefore, the corresponding unphysical cut or pole (left-hand cut in the dispersion relation) is called a dynamical cut, in contrast to the boundary, or unitary, cut. Unitarity imposes restrictions on only the right-hand cut, and if they are satisfied there, an amplitude satisfying the dispersion relation is automatically unitary. We shall describe the dynamics ourselves, establishing the discontinuity across the left-hand cut. We shall then see what is obtained in some concrete examples.

Dispersion relations were apparently first used for nuclear processes in Ref. 26, and in the same paper forward dispersion relations were used to calculate the amplitude of *nd* scattering. In this case the dynamical cut enters only from the graph of Fig. 1(a), i.e., it reduces to a pole at the point (3). In Ref. 26, the dispersion relation method was expounded in detail for complicated systems, and all the independent (with respect to the spin) amplitudes in *nd* scattering were calculated (five in all). As a result, it was shown that the forward dispersion relations in which one retains the contribution of two poles (from Fig. 1(a) and Fig. 13) and the right-hand unitary cut are consistent with the measured shift of *nd* scattering at one fixed energy. The agreement was excellent.

The most recent and most detailed investigation of the *nd* process by means of dispersion relations is Ref. 27. For the amplitude normalized in the usual manner:

$$\mathrm{Im} f(E) = k\sigma(E)/4\pi$$

and related to the doublet and quartet amplitudes by the zero-energy relation

$$\underset{E\to 0}{f}(E) = 2\,{}^4f(E)/3 + {}^2f(E)/2,$$

a forward dispersion relation was written down with one subtraction at zero energy:

$$\mathrm{Re} f(E) - f(0) = \frac{r_t E}{(E_t - E)E_t} + \frac{r_p E}{(E_p - E)E_p} + \frac{k^2}{2\pi^2}\int_0^{\infty} \frac{\sigma_{nd}(k')\, dk'}{k'^2 - k^2}. \tag{29}$$

Note that the energy is here measured in the center-of-mass system. The position of the triton pole corresponding to the graph (see Fig. 13) is given by

$$E_t = -(\epsilon_t - \epsilon) = -6.25\ \mathrm{MeV}.$$

The position of the pole in the graph (see Fig. 1(a)) is

$$E_p = -\epsilon/3 = -0.74\ \mathrm{MeV}.$$

In Eq. (29), the contribution of all singularities across the left-hand cut except those mentioned is ignored. Note that the graphs which are not reproduced by the dispersion relation (29) have very distant left-hand singularities. For example, the graph of Fig. 14 gives a singularity at $E \approx -70$ MeV, so that it would seem to be fully justified to ignore it in the subtracted dispersion relation. In Ref. 27, the procedure was reduced to selecting parameters r_t and r_p that describe the experiment best [$\mathrm{Re} f(E)$, $f(0)$, and $\sigma_{nd}(k)$ are taken from the experiment]. At the same time, r_p can be compared with the known vertex $d \to np$, while the vertex $T \to dn$ can be obtained from r_t. Excellent agreement was obtained for r_p and evidently the best value[27] for r_t. The

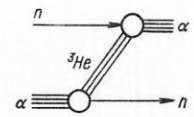

FIG. 15.

procedure for extracting r_t can be improved by using a conformal transformation,[28] as was done in Ref. 29. In the case of *nd* scattering, since the unsubtracted singularities are distant, a conformal transformation does not essentially affect the results.

Forward dispersion relations were also used for other scattering processes on nuclear systems (see, for example, the review Ref. 30). In order to illustrate the difficulties which arise in the general case, let us dwell on $n\alpha$ scattering, which was investigated in Refs. 31. Here there is qualitative and to some extent quantitative agreement with the $n\alpha$ scattering data, though the attempt to determine independently the vertex $\alpha \to {}^3\mathrm{He} + n$ at the pole corresponding to the graph in Fig. 15 failed. The reason for this was investigated in Ref. 29, in which it was shown that in this process, in contrast to *nd* scattering, the unsubtracted singularities lie near the pole of Fig. 15. For example, the singularity of Fig. 16 for the forward direction is at $E_{c.m} = -3(\epsilon_\alpha - \epsilon)/5 = 15.6$ MeV, whereas the pole diagram (see Fig. 15) gives a pole at $E_{c.m} = -3(\epsilon_\alpha - \epsilon_{^3\mathrm{He}})/5 \approx -12.3$ MeV. One therefore required[29] a more refined technique of conformal mapping[28] in order to extract data on the vertex $\alpha \to {}^3\mathrm{He} + n$. A similar technique was used in Ref. 32 for $p + {}^3\mathrm{He}$ scattering.

A different method, namely dispersion relations for partial waves, has an important difference, since it does not require the inclusion of experimental data. The total cross section in the forward dispersion relation is here simply replaced by the unitarity condition for the partial-wave amplitude. The dynamical cut is again determined by the graph with the nearest singularity. The N/D method is used to solve the inhomogeneous nonlinear integral equation obtained from the dispersion relation. This method was used successully in, for example, Ref. 33, in which *nd* scattering was investigated.

Using the variable $y = E/\epsilon$, one can represent the S wave of *nd* scattering, $f(y) = y^{-1/2}\exp(i\delta)\sin\delta$, in the form

$$f(y) = N(y)/D(y) \tag{30}$$

with the unitarity condition

$$\mathrm{Im}\, f(y) = \sqrt{y}\,|f(y)|^2 \tag{31}$$

and left-hand cut corresponding to the graph of Fig. 1(a). The contribution of this graph is

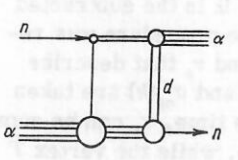

FIG. 16.

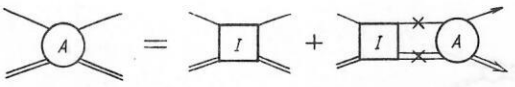

FIG. 17.

$$\Delta(y) = -\frac{2\gamma}{y\sqrt{3}}\ln\frac{1+3y}{1+y/3};\quad \gamma = (1 - r_{\mathrm{eff}} r_d)^{-1}. \tag{32}$$

Substitution of (30) into (31) and the dispersion relation give

$$D(y) = 1 - \frac{y}{\pi}\int_0^\infty \frac{\sqrt{x}\,N(x)\,dx}{x(x-y)};\quad N(y) = \frac{1}{\pi}\int_{-3}^{-1/3}\frac{D(x)\,\mathrm{Im}\,\Delta(x)\,dx}{x-y}. \tag{33}$$

Equations (33) can be solved analytically with an error of about 2—3%. Thus, the quartet length of *nd* scattering was obtained in Ref. 33 in good agreement with the experiment: $a_4 \approx 6.3$ F ($a_4^{\mathrm{exp}} = 6.17$ F).

Both the methods discussed above can be regarded as methods of iterating the simplest graph of Fig. 1(a) subject to the condition that the sum of the resulting series satisfies the unitarity condition; for we shall integrate the dispersion relation, taking this simplest graph as first approximation. Then, as is easily seen, we reproduce the complete series of *nd* scattering graphs, but with allowance for only the unitary cut Δ_5 determined in the foregoing section. In other words, all the intermediate states in the system, even in the virtual states, are present in *nd* but not *nnp* form. Three-particle intermediate states are taken into account for the forward dispersion relation, since the integral along the right-hand cut contains σ_{tot}, though here this cross section is taken from experiment and there is no closed iterative scheme. Of course, in all the dispersion relations discussed above the "anomalous" graphs of the type of Figs. 7 and 14 and all their iterations are rejected. Thus, the dispersion relations unitarize the principal graph for the process, and such an approximate unitarization (with contribution of the cut Δ_4 neglected) gives reasonable results at low energy.[33]

A different method of unitarization was considered by Sloan, Cahill, and their collaborators. For the scattering process the unitarization procedure was proposed by Sloan[7] and has the following form. From the two-particle t matrix, separate the pole term:

$$t(k, k', E) = -i\pi\varphi(k)\varphi(k')\delta(E+\varepsilon) + t^{(1)}. \tag{34}$$

Then $t^{(1)}$ serves to define the irreducible amplitude $I(\mathbf{kp}, \mathbf{k'p'}: z)$, which does not contain an intermediate *nd* state (there is no cut Δ_5 in the notation of the foregoing section). Then the equation for the amplitude $A(\mathbf{p}, \mathbf{p'}; z)$ of *nd* scattering has the form

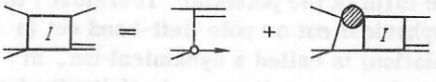

FIG. 18.

FIG. 19.

$$A(\mathbf{p}, \mathbf{p}'; z) = I(\mathbf{p}, \mathbf{p}'; z) - 2i\pi \int I(\mathbf{p}, \mathbf{p}''; z)\, A(\mathbf{p}'', \mathbf{p}'; z)\, \delta(3p''^2/4m - z + \varepsilon)\, d\mathbf{p}'' \quad (35)$$

and is represented graphically by Fig. 17, in which the crosses mean that the particles are on the energy shell. The equation for I has the graphical form shown in Fig. 18 [note that (35) contains I for $k = k' = i\alpha$, i.e., on the nd energy shell]. In Fig. 18 the hatched circle stands for $t^{(1)}$.

The three equations we have written down are exact, but as hard to solve as the exact Faddeev equation. The decisive step is the choice of an approximation for I; namely, one chooses the two first iterations (of course one could take more), i.e., the pole and triangular graph but with $t^{(1)}$ instead of t, as in Fig. 19. Using the explicitly known expression for I, it is not difficult to solve Eq. (35); for the partial waves the solution has the form

$$f_L = \frac{nI_L}{1 - inpI_L}; \quad n = -8\pi^2 m/3. \quad (36)$$

The approximate and exact solutions are compared in Figs. 20 and 21 at the energies $E_{1ab} = 1.3$ and 14.1 MeV, respectively. It can be seen how much approximate allowance for unitarity improves the agreement. Note an important fact. At low energies, the contribution of the first two graphs (see Figs. 1(a) and 1(b)) to the scattering exceeds the exact and experimental cross sections by many times: by 100 or more times at $E_{1ab} = 1.3$ MeV and by more than three times at $E_{1ab} = 14.1$ MeV. At the same time, if the same graphs are taken for I_L, and one then unitarizes them in accordance with (36), agreement between the exact and experimental values is recovered. The reason for this is clear from (36), since when nI_L becomes large (exceeding a certain limit, which can be called the unitary limit), f_L remains bounded—the unitarization mechanism renormalizes the graphs.

We now turn to breakup processes. Cahill and Sloan[12] proposed the following approximation scheme for the breakup amplitude B shown in Fig. 22. Note that the open circle now denotes the total t matrix, and that to obtain B it is first necessary to calculate A. Thus, the equation in Fig. 22 means one is taking into account interaction in the initial state—multiple scattering of a

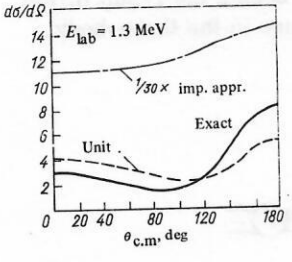

FIG. 20.

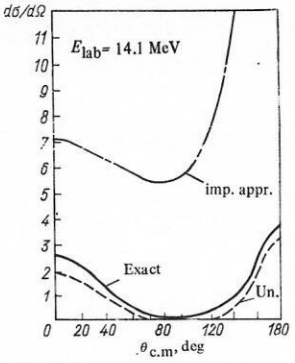

FIG. 21.

nucleon on the deuteron, but this is not the distorted-wave method in the literal sense, since the particles are on the energy shell and their interaction is not described by a potential. Figure 23 shows the proton spectrum in nd breakup for $\theta_L = 10°$ and $E_{n,1ab} = 14.4$ MeV: one curve is the solution of the equation in Fig. 22 in the same approximation for I as before; the other curve is the exact calculation for the Yamaguchi potential with allowance for the spin dependence.

It can be seen from Fig. 23 that the profile of the spectrum and the QFS peak are reproduced fairly well. With regard to the quantitative agreement, it is best illustrated by the following numbers. The first three approximations for I, i.e., the simplest pole graph, the same plus the triangular graph, and the sum of the first three graphs, give, respectively, 720, 1780, and 5120 mb for the breakup cross section. When elastic unitarity is taken in account in accordance with the equation in Fig. 22, the values 184, 142, and 161 mb are obtained with the same approximations for I. The exact value is 166 mb, which agrees excellently with the last number, but even the crudest approximation for I (the exchange diagram gives 184 mb) is only 10% greater than the exact value. Good agreement is also obtained in the region of the FSI peak (see Ref. 12).

Let us consider how well the unitarity conditions are satisfied in this approximation and what sequence of graphs is then reproduced. First, it can be seen that A and B do not contain the graphs shown in Figs. 24(a) and 24(b). Nevertheless, the unitarity condition for A is reproduced as follows: the elastic discontinuity Δ_5 is taken into account exactly, i.e., the unitarity condition leaves A in the framework of the adopted approximation. The discontinuity Δ_{4d}, corresponding to the inelastic cut, is also reproduced, but in this case B must be taken to be the collection of graphs in the same approximation as is given by the equation of Fig. 22. However, here the cut Δ_{4n} is completely absent. This cut could appear in the graph shown in Fig. 25 if all the particles on the section with the wavy line were on the energy shell. But this is impossible since the deuteron in

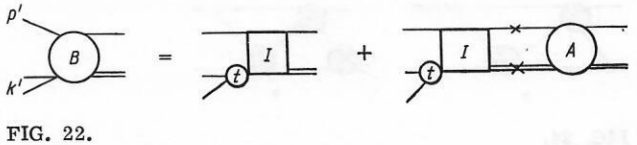

FIG. 22.

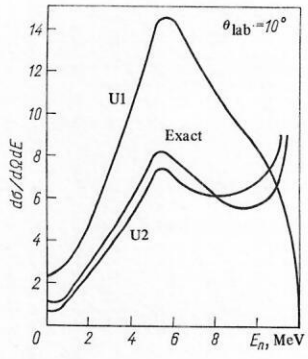

FIG. 23.

Fig. 25 is already on the energy shell, and therefore cannot decay into two free nucleons. All that we have said can be literally repeated for the breakup amplitude B. Thus, we see that even partial allowance for the requirements of unitarity (correct discontinuity across the elastic cut) leads not only to qualitative but also reasonable quantitative agreement with experiment. The solution of the equations in Figs. 17 and 22 does not even require integration, since they are algebraic.

A completely unitarized amplitude was constructed in Refs. 13 and 15 by a consistent stepwise scheme. The corresponding equations are represented graphically in Figs. 26–29, in which one integrates with allowance for the conservation laws over all intermediate states and the particles are taken onto the energy shell (this last is indicated by the dashed line intersecting the internal lines of the graphs). Cahill and Kowalski[13,15] start from an arbitrarily given function F, which need not have the cuts $\Delta_1-\Delta_5$ (it may have left-hand cuts). Then the equation in Fig. 26 gives the amplitude Q, which satisfies the requirements of elastic two-particle unitarity. Note that if F is identified with I, the equation in Fig. 26 immediately gives the elastic amplitude A, since it coincides with the equation in Fig. 17. Substituting the resulting Q into the equation in Fig. 27, we construct the amplitude N, which has not only the correct discontinuity Δ_5 across the cut but also the discontinuities Δ_{4d} and Δ_{3d}. We then substitute N into the equation in Fig. 28 and already obtain the breakup amplitude B, which now has the correct unitary properties across the discontinuities Δ_{3n} and Δ_{4n}. The elastic amplitude is then obtained by means of the equation in Fig. 29. Note that R in the equation in Fig. 27 is the two-particle R matrix, which is related to the T matrix by the usual equation:

$$T=R-i\pi R\delta(H_0-E)T. \tag{37}$$

Thus, the scheme gives us amplitudes A and B satisfying all the unitary properties except one—the dynamical discontinuity Δ_1 is not reproduced since F by

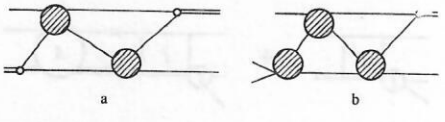

FIG. 24.

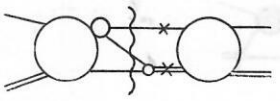

FIG. 25.

its choice should not have singularities there. None of the other quantities can have the cut Δ_1, since they contain only higher iterations of F. For the same reason, the unitarity condition for the amplitude $w(3\to 3)$ is not satisfied; however, this may not be so important for A and B since w occurs in them only indirectly, through the unitarity condition.

In practice, F can be taken to be the simplest graph, the pole graph, but in it one must eliminate the singularity Δ_1, for which the graph must be taken in the principal value sense. Specifically, in Ref. 14 the graph shown in Fig. 30, in which the circles (vertices) correspond to R matrices and the bar across the nucleon line means that the δ function must be omitted, was selected. Then the solution of the equations in Figs. 26–29, after expansion with respect to partial waves, reduces to the solution of a system of one-dimensional integral equations instead of the two-dimensional equations in the exact Faddeev method. The results of the calculations of Ref. 14 are given in Fig. 31 for elastic scattering at 14.4 MeV and are compared with the simple unitarization (36) and the exact calculation for the Yamaguchi potential. It can be seen that the more accurate fulfillment of the unitarity conditions leads to a better quantitative agreement. However, a shortcoming of the method is its complexity—the result cannot be obtained in analytical form but only numerically, as a result of successive solution of a system of equations. Therefore, the practical expediency of the method, in particular for more complicated systems than the deuteron, is in doubt. Nevertheless, this is the first method in which three-particle inelastic unitarity has been taken into account exactly (for the discontinuity Δ_4).

A different method of unitarization by means of the introduction of the three-particle K matrix was proposed in Ref. 34 and used to calculate resonances in a three-body system in Ref. 35. In this paper, the K matrix was introduced very formally, and one can show that the unitarity conditions are satisfied only if the K matrix satisfies an exact equation which is as complicated as Faddeev's. But if the Hilbert-Schmidt expansion is used for the K matrix and a finite number of terms retained, as in Ref. 34, the unitarity conditions are violated. Another shortcoming of Ref. 34 is that the eigenvalues $\Lambda_n(E)$ introduced there are not analytical functions of the energy. Because of this, one doubts the result of Ref. 35, which predicted a resonance in the three-body system.

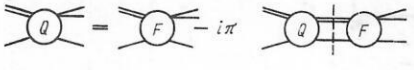

FIG. 26.

FIG. 27.

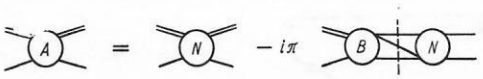

FIG. 29.

In Sec. 4 we shall propose a different approach to the construction of unitarized amplitudes.

4. THE HILBERT-SCHMIDT METHOD FOR THREE PARTICLES

Hilbert-Schmidt Method and its Physical Interpretation: The Example of Two Particles. For $2 \to 2$ reactions, the method known usually as R-matrix theory has long been used. In the general many-channel case, this method enables one to write down phenomenologically an S matrix that satisfies the following requirements: a) two-particle unitarity; b) correct threshold behavior near the two-particle thresholds; c) appearance of resonances which decay into two particles (subsystems). Below, we shall set forth a different approach—the Hilbert-Schmidt method, which can be regarded as either a phenomenological (if one wishes) or a dynamical approach to the calculation of all the characteristics of the process, including the parameters of resonances. In the last case, the Hilbert-Schmidt method is the only mathematically consistent method that enables one to determine the wave function of a resonance. It is important that the Hilbert-Schmidt method enables one to describe a system of two, three, four, etc., subsystems, and the description of two particles by the Hilbert-Schmidt method is then used to consider a system of three particles, four particles, and so forth. Here we shall present the method as applied to three-particle systems. The principal result and advantage of the method is that the t matrix on and off the energy shell is represented as a sum over discrete states—poles which correspond to virtual or bound states or resonances, and this sum converges rapidly.

For two particles, it is convenient to formulate the method[36] on the basis of the Lippmann-Schwinger equation:

$$(p^2/m - E)\,\psi(\mathbf{p}) = -\int V(\mathbf{p}-\mathbf{p}')\,\psi(\mathbf{p}')\,d\mathbf{p}'. \tag{38}$$

Introducing the vertex function $a(\mathbf{p}, E) = (p^2/m - E)\psi(\mathbf{p})$, let us consider the solutions of the homogeneous equation obtained from (38):

$$a_\nu(\mathbf{p}, E) = -\frac{1}{\mu_\nu(E)}\int \frac{V(\mathbf{p}-\mathbf{p}')\,a_\nu(\mathbf{p}', E)}{(p'^2/m - E)}\,d\mathbf{p}'. \tag{39}$$

Equation (39) is an equation of Fredholm type for $E<0$ and, moreover, the kernel of an equation of Hilbert-Schmidt type. For all the remaining E off the cut $E \geqslant 0$, the solutions and eigenfunctions $\mu_\nu(E)$ are obtained by analytic continuation in E from the region $E<0$, where the set $\mu_\nu(E)$ is discrete and does not have accumulation points. Moreover, the set $a_\nu(\mathbf{p}, E)$ forms a complete system for expansion and operation of all operators which are determined by kernels expressed in terms of the kernel of Eq. (39). For example, the equation for the t matrix has the form

$$t(\mathbf{p}, \mathbf{p}'; z) = V(\mathbf{p}-\mathbf{p}') - \int \frac{V(\mathbf{p}-\mathbf{p}'')\,t(\mathbf{p}'', \mathbf{p}'; z)}{(p''^2/m - z)}\,d\mathbf{p}''. \tag{40}$$

It can be seen from this that t can be expressed in terms of the resolvent of Eq. (39) and can therefore be expanded with respect to $a_\nu(\mathbf{p}, z)$.

As usual, we write down for an equation of Hilbert-Schmidt type an expansion of the kernel:

$$V(\mathbf{p}-\mathbf{p}') = -\sum_\nu \mu_\nu a_\nu(\mathbf{p}, z)\,a_\nu(-\mathbf{p}', z). \tag{41}$$

Then

$$t(\mathbf{p}, \mathbf{p}'; z) = -\sum_\nu \frac{\mu_\nu(z)}{1-\mu_\nu(z)}\,a_\nu(\mathbf{p}, z)\,a_\nu(-\mathbf{p}', z). \tag{42}$$

The functions $a_\nu(\mathbf{p}, z)$ satisfy the normalization

$$\int \frac{a_\nu(\mathbf{p}, z)\,a_{\nu'}(-\mathbf{p}, z)}{(p^2/m - z)}\,d\mathbf{p} = \delta_{\nu\nu'}. \tag{43}$$

For a centrally symmetric potential it is convenient to separate out in $a_\nu(\mathbf{p}, z)$ the explicit dependence on the angle [and accordingly from the index (ν) separate out the quantum numbers l and m]:

$$a_\nu(\mathbf{p}, z) = a_{\nu l}(p, z)\,Y_{lm}(\mathbf{p}/p), \tag{44}$$

and for $t_l(p, p'; z)$ we then obtain

$$t_l(p, p'; z) = -\frac{1}{4\pi}\sum_\nu \frac{\mu_{\nu l}(z)}{1-\mu_{\nu l}(z)}\,a_{\nu l}(p, z)\,a_{\nu l}(p', z), \tag{45}$$

and the normalization condition for $a_{\nu l}(p, z)$ is

$$\int \frac{a_{\nu l}(p, z)\,a_{\nu' l}(p, z)}{(p^2/m - z)}\,p^2\,dp = \delta_{\nu\nu'}. \tag{46}$$

The Hilbert-Schmidt eigenvalues $\mu_{\nu l}(z)$ depend on l, although in what follows this index will be always omitted for simplicity. The kernel of Eq. (39) being real for $E<0$, it follows that $\mu_\nu(E)$ is a real analytic function for an Hermitian potential V:

$$\mu_\nu(z^*) = \mu_\nu^*(z). \tag{47}$$

In addition, taking the lth partial wave of Eq. (39), we find that[36]

$$a_{\nu l}(p, z) \sim p^l, \tag{48}$$

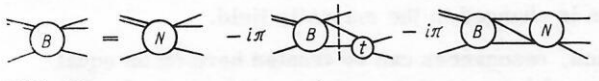

FIG. 28.

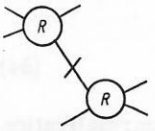

FIG. 30.

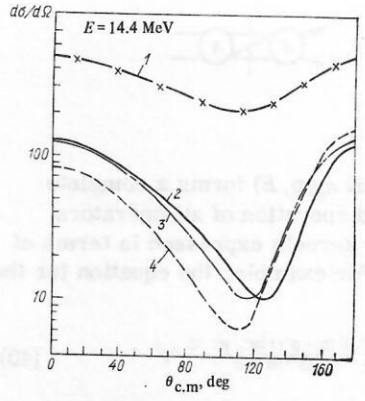

FIG. 31. 1) impulse approximation; 2) exact calculation; 3) unitarization of the simplest graph; 4) quasiunitarization of the two first graphs by Sloan's method.

and also that

$$\mu_{\nu,\,l}(z) \underset{z\to 0}{\sim} z^{l+1/2}; \tag{49}$$

$$a_{\nu l}(p,\, z^*) = a^*_{\nu l}(p,\, z). \tag{50}$$

It can be seen from (49) that it is convenient to introduce the variable $k=\sqrt{mz}$ and consider $\mu_{\nu l}(k)$ on the whole of the k plane; then $\mu_{\nu l}(k)$ is an analytic function of k everywhere in the upper half-plane of k. The elements of the S matrix can be expressed in terms of $\mu_{\nu l}(k)$ directly[16,36]:

$$S_l(k) = \prod_{\nu=1}^{\infty} \frac{1-\mu_{\nu l}(-k)}{1-\mu_{\nu l}(k)}. \tag{51}$$

It can be seen from (45) that a tending of $\mu_\nu(z)$ to unity at some negative z means a pole in the t matrix, while a tending to unity at a complex point $z=z_0=E_0-i\Gamma/2$ gives the Breit-Wigner resonance formula. Then $a_\nu(p,z)$ [or rather $\psi_\nu(p,z)$] are, respectively, the wave functions of the bound state and the resonance in the two-particle system. In order to understand better the physical meaning and significance of our result, let us go over to coordinate space. We write down the equation equivalent to (38) and (39):

$$\left[H_0+\frac{1}{\mu_\nu(E)}V(r)\right]\psi_\nu(r,\, E) = E\psi_\nu(r,\, E). \tag{52}$$

The boundary conditions follow from the homogeneous equation (39) for $E=E+i\delta$, $\delta>0$:

$$\left.\begin{aligned} &\psi_\nu(r,\, E) \text{ finite at zero}\\ &\psi_\nu(r,\, E) \to \exp(ikr)/r,\ r\to\infty. \end{aligned}\right\} \tag{53}$$

It can be seen from this that when $\operatorname{Im} k>0$ one must take an asymptotically decreasing, and therefore normalized solution. The normalization condition for the function $\psi_\nu(r,E)$ corresponding to (46) is

$$\int \psi_\nu(r,\, E)\, V(r)\, \psi_{\nu'}(r,\, E)\, d\tau = -\mu_\nu \delta_{\nu\nu'}. \tag{54}$$

For $E<0$ there also exists the ordinary normalization integral, because $\mu_\nu(E_0)=1$ determines a bound state at the point E_0 and $\mu_\nu^{-1}(E)$ itself shows by how many times the potential must be deepened in order that a νth level arise at the energy E.

One can immediately establish how rapidly the $\mu_\nu(E)$ decrease with increasing ν by taking a finite-range potential and noting that qualitatively the picture in such a potential does not differ from that for the potential of a rectangular well, and that the situation in a sufficiently deep well ($\nu\to\infty$) does not differ from that in an infinitely deep one if the energy is measured from the bottom of the well. In such a well of radius R, the energy of level ν is given by

$$E_\nu = \hbar^2\pi^2\nu^2/(mR^2).$$

Hence, going over to measuring the energy from zero, as usual, we obtain

$$|V_0|/[\mu_1(E)] = |E| + \hbar^2\pi^2/(mR^2) \text{ and } |V_0|/[\mu_\nu(E)] = |E| + \hbar^2\pi^2\nu^2/(mR^2). \tag{55}$$

From (55) we readily find

$$\mu_\nu(E) = |V_0|/[|E| + \hbar^2\pi^2\nu^2/(mR^2)]. \tag{56}$$

Thus: 1) $\mu_\nu(E)$ decreases as $1/\nu^2$; 2) the decrease as $\nu\to\infty$ begins when $\nu\gg\nu_0$, where $\nu_0^2 \sim mR^2|E|/(\hbar^2\pi^2)$, i.e., with increasing energy it is protracted; 3) $\mu_\nu(E)$ for fixed ν decreases with increasing $|E|$ as $1/|E|$. By virtue of the analyticity of $\mu_\nu(E)$, this property must be preserved as $|E|\to\infty$ along any ray. Because of the decrease $\mu_\nu \sim 1/\nu^2$ there is also decrease of the wave function ψ_ν on account of the normalization condition (54). Then the vertex functions $a_\nu(p,E)\sim 1$ as $\nu\to\infty$ as well and the complete series for the t matrix converges even faster; the successive terms in Eq. (45) decrease as $1/\nu^4$. This is extremely important for practical applications of the Hilbert-Schmidt method.

We now turn to $E>0$. Note that the asymptotic condition (53) and the normalization condition (54) are analytic in the energy and can also be used when $E>0$, in contrast to the ordinary normalization condition $\int|\psi|^2 d\tau = 1$. Therefore, for the resonance $E=E_0-i\Gamma/2$ one can use $\psi_\nu(r,E_0)$ as the wave function of the resonance. For example, the shift in the position of the resonance as a result of the perturbation $V_1(r)$ is given by the equation[37]

$$\Delta E = \int V_1(r)\,[\psi_\nu(r,\, E_0)]^2\, d\tau \Big/ \int [\psi_\nu(r,\, E_0)]^2\, d\tau. \tag{57}$$

Here the integral in the denominator of (57) converges for $E_0=E_0+i\delta$, $\delta\to 0$, i.e., in the usual physical limit.

The wave function $\psi_\nu(r,E)$ also determines the mean values of the operators; for example, for the magnetic moment of the resonance we obtain

$$\langle \mathfrak{M}_\nu \rangle = \operatorname{Re} \frac{\int \psi_\nu(r,\, E)\, \hat{\mathfrak{M}} \psi_\nu(r,\, E)\, d\tau}{\int [\psi_\nu(r,\, E)]^2\, d\tau}. \tag{58}$$

The symbol of the real part removes the imaginary correction, which arises because the width of the resonance is changed in the magnetic field.

Thus, resonances can be treated here on an equal footing with bound states. For an energy $E>0$, the

boundary condition (53) presupposes that the particles are created by the potential $V(r)/\mu_\nu(E)$, and therefore $\mathrm{Im}[V(r)/\mu_\nu(E)]>0$. For a real attractive potential, $V(r)<0$, it follows that $\mathrm{Im}\,\mu_\nu(E)>0$ for $E>0$. On the other hand, if the potential $V(r)$ takes into account inelastic absorption as, for example, in the case of the potential of a black sphere, we have $\mathrm{Im}\,V(r)<0$ and then $\mu_\nu(E)(E>0)$ must have $\mathrm{Im}\,\mu_\nu(E)>0$ *a fortiori*. However, for complex potentials the condition (47) is violated, and therefore $\mu_\nu(E-i\delta)=\mu_\nu(-k)$, which enters the expression (51) for the S matrix, may be real and equal to unity. Then $S_l(k)=0$, which corresponds to a perfectly absorbing sphere. Note that in the case of complex potentials for which the imaginary and real parts have the same form $\mu_\nu(E)$ is redefined in a simple way: $\mu_\nu(E)=\tilde{\mu}_\nu(E)(\mathrm{Re}\,V+i\,\mathrm{Im}\,V)/\mathrm{Re}\,V$, where $\tilde{\mu}_\nu(E)$ is the solution for a real potential. Different cases of explicitly solvable potentials for the determination of $\mu_\nu(E)$ are given in Ref. 38. If the potential has an infinite repulsive core, then the method is modified simply.[39] Some of the questions touched upon here have been considered in more detail in Refs. 17, 36—38, 40.

Hilbert-Schmidt Representation for Three-Particle Amplitudes. For a three-particle system described by the Faddeev equation[5] one can apply Hilbert-Schmidt theory consistently since this equation is of Fredholm type. If, as before, we restrict ourselves to the case when the pair of interacting particles has zero relative orbital angular momentum, $l=0$, and the Hilbert-Schmidt expansion (45) is used for the two-particle t matrix, we can represent the eigenfunction $\chi_n(k,\mathbf{p})$ of the homogeneous Faddeev equation with eigenvalue $\gamma_n(z)$ in the form[41]

$$\chi_n^L(k,\mathbf{p})=\frac{m\gamma_n(z)}{2\pi}\sum_\nu\frac{\mu_\nu(\varkappa)}{1-\mu_\nu(\varkappa)}a_\nu(k,\varkappa^2/m)\,\tilde{b}_{\nu n}^L(\mathbf{p},z). \tag{59}$$

Here

$$\varkappa^2=mz-3p^2/4;\quad z=E+i\delta. \tag{60}$$

For the chosen $l=0$, the total angular momentum of the system is equal to the third particle's: L. In the functions $\tilde{b}_{\nu n}^L(\mathbf{p},z)$ it is convenient to separate the angular dependence:

$$\tilde{b}_{\nu n}^L(\mathbf{p},z)=Y_{LM}(\mathbf{p}\,p)\,b_{\nu n}^L(p,z). \tag{61}$$

Then $b_{\nu n}^L(p,z)$ are solutions of the homogeneous Faddeev equation:

$$b_{\nu n}^L(p,z)=\gamma_n(z)\sum_{\nu'}\int\mathscr{K}_{\nu\nu'}^L(p,p';z)\,b_{\nu' n}^L(p',z)\,p'^2\,dp', \tag{62}$$

where the kernel of the equation is

$$\mathscr{K}_{\nu\nu'}^L(p,p';z)=m\int\frac{d\cos\theta P_L(\cos\theta)}{(p^2+\mathbf{pp}'+p'^2-mz)}\frac{\mu_{\nu'}(\varkappa')}{[1-\mu_{\nu'}(\varkappa')]}a_\nu\left(\left|\frac{\mathbf{p}}{2}+\mathbf{p}'\right|,\frac{\varkappa^2}{m}\right)\times a_{\nu'}\left(\left|\frac{\mathbf{p}'}{2}+\mathbf{p}\right|,\frac{\varkappa'^2}{m}\right); \tag{63}$$

$$\theta=\widehat{\mathbf{pp}'},\quad \varkappa'^2=mz-3p'^2/4.$$

The eigenfunctions of Eq. (62) satisfy the normalization condition

$$\sum_\nu\int b_{\nu n}^L(p,z)\,b_{\nu n'}^L(p,z)\frac{\mu_\nu(\varkappa)}{1-\mu_\nu(\varkappa)}\,p^2\,dp=\delta_{nn'}, \tag{64}$$

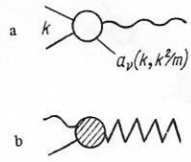

FIG. 32.

and the kernel of Eq. (62) can be expanded in the usual manner in the eigenfunctions $b_{\nu n}^L(p,z)$.

The important point for what follows is that the $3\to3$ amplitude $w(k\mathbf{p},k'\mathbf{p}';z)$ can, as can be seen from Eq. (8) and was shown in Refs. 16 and 17, be represented in the form

$$w(k\mathbf{p},k'\mathbf{p}';z)=\frac{1}{4\pi}\sum_{\nu\nu'}\frac{\mu_\nu(\varkappa)\,a_\nu(k,\varkappa^2/m)\,\mu_{\nu'}(\varkappa')\,a_{\nu'}(k',\varkappa'^2/m)}{[1-\mu_\nu(\varkappa)]\,[1-\mu_{\nu'}(\varkappa')]}\times w_{\nu\nu'}(\mathbf{p},\mathbf{p}';z), \tag{65}$$

where the function $w_{\nu\nu'}(\mathbf{p},\mathbf{p}';z)$ satisfies an inhomogeneous equation[25] whose kernel in fact is identical with (63), and the partial-wave amplitude $w_{\nu\nu'}^L(p,p';z)$ is in fact the resolvent of Eq. (62). It therefore has the expansion

$$w_{\nu\nu'}^L(p,p';z)=\frac{1}{4\pi}\sum_n\frac{b_{\nu n}^L(p,z)\,b_{\nu' n}^L(p',z)}{1-\gamma_n(z)}. \tag{66}$$

Here the partial-wave amplitude $w_{\nu\nu'}^L(p,p';z)$ can be expressed in terms of the total amplitude $w_{\nu\nu'}(\mathbf{p},\mathbf{p}';z)$ [the expression (65)] in the usual way:

$$w_{\nu\nu'}(\mathbf{p},\mathbf{p}';z)=\sum_L(2L+1)\,P_L(\cos\theta)\,w_{\nu\nu'}^L(p,p';z). \tag{67}$$

From Eqs. (65) and (66) and the definition of the scattering and breakup amplitudes, one can readily obtain the Hilbert-Schmidt representation for the amplitudes A and B. To be specific we shall assume that the eigenvalue $\nu=\nu_0$ corresponds to the deuteron pole. Near the pole, we have the expansion $\mu_{\nu 0}(z)=1+\mu'_{\nu 0}(-\epsilon)\times(z+\epsilon)$ and the function $\varphi(\alpha)=a_{\nu 0}(i\alpha,\ -\epsilon)/\sqrt{\mu'_{\nu 0}(-\epsilon)}$ is the deuteron wave function ($\alpha^2=m\epsilon$) in the usual normalization when $t(k,k';z)=\varphi(k)\,\varphi^*(k)/[4\pi(z+\epsilon)]+\cdots$. As a result, we obtain the following Hilbert-Schmidt expansion for the partial-wave amplitudes[17]:

$$A_L(p,z)=\frac{1}{4\pi\mu'_{\nu_0}(-\epsilon)}\sum_n\frac{[b_{\nu_0 n}^L(p,z)]^2}{1-\gamma_n(z)} \tag{68}$$

and

$$B_L(p,k'p';z)=\frac{(-1)}{\sqrt{4\pi\mu'_{\nu_0}(-\epsilon)}}\sum_n\sum_\nu\frac{\mu_\nu(k')\,a_\nu(k',k'^2/m)}{[1-\mu_\nu(k')]}\frac{b_{\nu_0 n}^L(p,z)\,b_{\nu n}^L(p',z)}{4\pi\,[1-\gamma_n(z)]}. \tag{69}$$

Note also that the inhomogeneous term of Eq. (8), which we denote by $w^{(0)}(k\mathbf{p},k'\mathbf{p}';z)$, allows a repre-

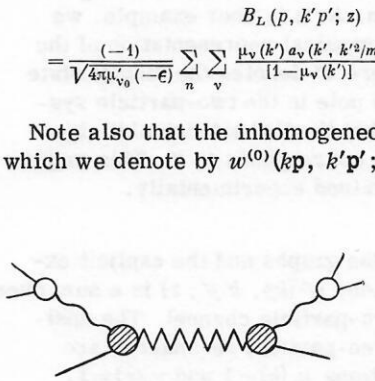

FIG. 33.

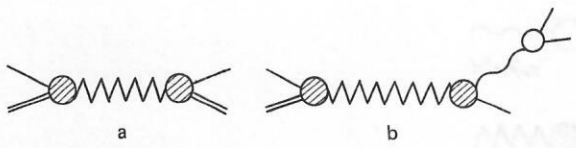

a b

FIG. 34.

sentation in the form (65), and that its partial-wave amplitude $w^{(0)L}_{\nu\nu'}(p,p';z)$ has the expansion

$$w^{(0)L}_{\nu\nu'}(p,p';z)=\frac{(-1)}{4\pi}\sum_n \frac{1}{\gamma_n(z)} b^L_{\nu n}(p,z)\, b^L_{\nu' n}(p',z). \qquad (70)$$

Graphical Representation and Analytic Properties of the Hilbert-Schmidt Series. Above, we have represented the physical scattering and breakup amplitudes in the form of the Hilbert-Schmidt series. With each term of this series one can associate a simple graph, it being important that all the graphs have the same representation and differ only by the dependence of the vertices and the propagators on the indices ν and n.

We shall represent the external lines corresponding to observed particles by a continuous line; the observed deuteron, by two lines. The graphical representation will be based on the following identifications:

1) the two-particle vertex corresponds to the function $a_\nu(k, k^2/m)$, and will be denoted by a complete circle, as in Fig. 32(a);

2) $\mu_\nu(k)/[1-\mu_\nu(k)]$ acquires the meaning of a propagator, and will be represented by a wavy line. We shall say that the wavy line corresponds to the propagation of an eigeon with index ν;

3) we associate the three-particle vertex with the function $b^L_{\nu n}(p,z)$ and represent it by a hatched circle (see Fig. 32(b)). A particle line and a line of a two-particle eigeon enter this vertex and the zig-zag line of the three-particle eigeon leaves it;

4) the four-particle propagator takes the values $[1-\gamma_n(z)]^{-1}$, and we shall represent it by a zig-zag line. This line corresponds to the propagation of a three-particle eigeon.

Thus, to each term of the series for the $3\to 3$ partial-wave amplitude $w^L(kp, k'p'; z)$ there corresponds the graph shown in Fig. 33. The elastic scattering amplitude A_L is represented as the sum of the graphs shown in Fig. 34(a). We recall that the eigenvalue $\nu=\nu_0$ corresponds to the deuteron. As a further example, we show in Fig. 34(b) the graphical representation of the $nd\to nd^*$ amplitude, where d^* denotes the singlet state of a deuteron—a virtual pole in the two-particle system. We shall assume that the Hilbert-Schmidt eigenvalue with number $\nu=\nu_1$ corresponds to it. This amplitude is frequently determined experimentally.

As can be seen from the graphs and the explicit expression for the amplitude, $w^L(kp, k'p'; z)$ is a sum over the resonances in the two-particle channel. The positions of the two- and three-particle resonances are determined by the conditions $\mu_\nu(k)=1$ and $\gamma_n(z)=1$, respectively. The question of three-particles resonances is discussed in detail in Sec. 6. Here, we merely emphasize that all the singularities of the amplitude w except the dynamical cut are reproduced by each term of the sum. Namely, the FSI cuts arise in (65) because of the singularities of the functions $a_{\nu'}$ and $\mu_{\nu'}$, which depend on the momenta k' and p' in the final state, and also of the functions $b_{\nu n}(p', z)$.

The elastic $(-\epsilon, \infty)$ and three-particle $(0, \infty)$ unitary cuts arise solely from the functions $b_{\nu n}(p,z)$ and $\gamma_n(z)$. With regard to the dynamical cut, the situation here is the same as when allowance is made for the potential cut in the two-particle t matrix in the Hilbert-Schmidt expansion. It is well known that a finite number of terms in (45) does not contain the left-hand potential cut. However, for the energy values $E>-\epsilon$ of interest to us, this cut is in the unphysical region and the t matrix is reproduced to a high numerical accuracy by the first few terms. It is important[17] that the successive terms of the series decrease as $1/\nu^4$. Similarly, in the three-particle scattering and breakup amplitude the dynamical cut is in the unphysical region,[25] and it is therefore sufficient to reproduce numerically with good accuracy the values of the amplitudes for energies $E>-\epsilon$. In fact we have already shown that the eigenvalues $\gamma_n(z)$ increase with n as n^2, and therefore the Hilbert-Schmidt series for the three-particle amplitudes decreases at least as $1/n^2$. This presupposes that the first few terms reproduce numerically with high accuracy the three-particle physical characteristics.

Indeed, the first numerical calculations[42] showed that the nd scattering length in the spinless case and for the quartet state is determined by the first three terms with an error not worse than 5%, and the second eigenvalue γ_2^{-1} is about five times smaller than γ_1^{-1}. It is true that the situation worsens in calculations of the doublet nd scattering length, for which five terms are required to achieve the same accuracy.[42] The slowing down of the convergence of the Hilbert-Schmidt series in this case is due to the small absolute value of the doublet scattering length, and although γ_2^{-1} is approximately 3.5 times less than γ_1^{-1}, they make contributions of opposite signs, and the first two terms of the Hilbert-Schmidt series cancel strongly.

We should also like to emphasize that if for some physical reasons the dynamical singularity is very important, for example, at high energies $E\gtrsim 100$ MeV, it can be separated out explicitly. For this, we note that the entire dynamical singularity is contained in the inhomogeneous term of Eq. (8), which admits the Hilbert-Schmidt expansion (70). If to the amplitude $w^L_{\nu\nu'}(p,p';z)$ (66) we add and subtract the term $w^{L\,(0)}_{\nu\nu'}$, we obtain

$$w^L_{\nu\nu'}(p,p';z)=w^{(0)L}_{\nu\nu'}(p,p';z)+\frac{1}{4\pi}\sum_n \frac{b^L_{\nu n}(p,z)\, b^L_{\nu' n}(p',z)}{\gamma^L_n(z)[1-\gamma^L_n(z)]}. \qquad (71)$$

After the separation of the dynamical singularity, the sum over n in (71) decreases faster than the original series, since it contains the additional factor $\gamma_n(z)$, which increases as n^2 for large n.

Let us also dwell briefly on the main analytic properties of the three-particle eigenfunctions and eigenvalues. In Ref. 41 it was shown that

$$\gamma_n(z^*)=\gamma_n^*(z);\ b_{\nu n}^L(p,z^*)=b_{\nu n}^{L*}(p,z). \tag{72}$$

Near $p\to 0$

$$b_{\nu n}^L(p,z)\sim p^L,\ p\to 0. \tag{73}$$

The function $\gamma_n(z)$ has characteristic singularities at the two- ($z=-\epsilon$) and three-particle ($z=0$) thresholds.[17] Near $z=-\epsilon$, the function $\gamma_n(z)$ has an ordinary root singularity [like the two-particle eigenvalues $\mu_{\nu l}(k,E)$ near $E=0$]:

$$\gamma_n^L(z)\sim(z+\epsilon)^{L+1/2}. \tag{74}$$

At the point $z=0$, from which the three-particle unitary cut begins, $\gamma_n^L(z)$ has a logarithmic singularity:

$$\gamma_n^L(z)\sim z^{2-L}\ln z,\ z\to 0. \tag{75}$$

For the three-particle eigenfunctions $b_{\nu n}^L(p,z)$ in the region $z<0$ one can establish the sum rule[16]

$$1=\frac{4\pi i m p}{3\mu'_{\nu_0}(-\epsilon)}\sum_n\frac{|b_{\nu_0 n}^L(p,z)|^2}{1-\gamma_n(z)\,[\gamma_n(z^*)]^{-1}},\quad m=1,2,\ldots, \tag{76}$$

which holds for all m. Solving the system of algebraic equations (76), one can obtain for the S_L matrix the representation

$$S_L=\prod_{n\ 0}^{\infty}\frac{1-\gamma_n^L(z_-)}{1-\gamma_n^L(z_+)}. \tag{77}$$

Here, z_+ and z_- are the values of the energy on the upper and lower edges of the two-particle cut beginning at the point $z=-\epsilon$. For $z<0$, in accordance with (72), $\gamma_n(z_-)=\gamma_n^*(z_+)$, and therefore for each term in (77)

$$\left|\frac{1-\gamma_n(z_-)}{1-\gamma_n(z_+)}\right|=1,\quad z<0. \tag{78}$$

i.e., the representation (78) automatically ensures unitarity.

If the two-particle cut is now directed above the three-particle cut, Eq. (77) can be analytically continued to $z>0$ as well. The value z_- must be chosen at a point between the two cuts. Then (77) takes into account only the elastic part of the discontinuity of $\gamma_n(z)$ and $\gamma_n(z_-)\neq\gamma_n^*(z_+)$ for $z>0$. One can show that at the same time $|S_L|<1$.

Unitarity Conditions in the Hilbert-Schmidt Representation. Having represented the three-particle amplitudes as a Hilbert-Schmidt expansion, we can once more reformulate the unitarity conditions and study their consequences. Let us first consider only the untary cuts, i.e., the discontinuities Δ_4 and Δ_5: $\Delta_u=\Delta_4+\Delta_5$. It is easy to show[17] that the unitary condition reduces to the form

$$\Delta_u\sum_n\frac{b_{\nu n}^L(p,z)\,b_{\nu' n}^L(p',z)}{1-\gamma_n^L(z)}=-i\pi m\sum_{n,n'}\frac{b_{\nu n}^L(p,z)\,b_{\nu' n'}^L(p',z^*)\,M_{nn'}^L(z)}{[1-\gamma_n(z)]\,[1-\gamma_{n'}(z^*)]}, \tag{79}$$

where

$$M_{nn'}^L(z)=\frac{4p_0}{3\mu'_{\nu_0}(-\varepsilon)}\,b_{\nu_0 n}^L(p_0,z)\,b_{\nu_0 n'}^L(p_0,z^*)+\int_0^{\infty}p_1^2dp_1\sqrt{mz-3p_1^2/4}\,f_n(p_1,z)\,f_{n'}(p_1,z^*)$$
$$\times\theta(mz-3p_1^2/4)+2\int\int p_1\,dp_1p_2\,dp_2f_n(p_1,z)\,f_{n'}(p_2,z^*)\times P_L\left(\frac{mz-p_1^2-p_2^2}{p_1p_2}\right)\theta\left[1-\frac{|mz-p_1^2-p_2^2|}{p_1p_2}\right]. \tag{80}$$

Here $p_0^2=4(mz+m\epsilon)/3=4(mz+\alpha^2)/3$;

$$f_n(p_i,z)=\sum_\nu\frac{\mu_\nu(\varkappa_i)}{1-\mu_\nu(\varkappa_i)}a_\nu(\varkappa_i,\varkappa_i^2/m)\,b_{\nu n}(p_i,z) \tag{81}$$

and, as usual, $\varkappa_i^2=mz-3p_i^2/4$.

What can we say about the unitarity condition (79)? It is clear that if the eigenfunctions $b_{\nu n}^L(p,z)$ and the eigenvalues $\gamma_n^L(z)$ are an exact solution of Faddeev's equation, the unitarity conditions must be satisfied automatically. Nevertheless, this relation can be helpful and important, first, to establish the principal singularities and the analytic properties of the functions $b_{\nu n}^L(p,z)$ and $\gamma_n(z)$ and, second, to construct phenomenological functions satisfying these relations. Further, we see that the unitarity conditions in the form (79) establish only the connection between $\gamma_n(z)$ and $b_{\nu n}(p,z)$ and do not impose restrictions on the choice of $b_{\nu n}(p,z)$ if they are regarded as certain phenomenological functions.

Hitherto we have taken into account only the unitary discontinuities Δ_4 and Δ_5 of the amplitudes. We have already pointed out that the scattering amplitude A has only unitary cuts, but the breakup amplitude B has in addition the FSI cut beginning at the point $z_{f'}=3p'^2/4m$. This discontinuity is made up of the discontinuities Δ_{3d} and Δ_{3n} (12) and imposes additional restrictions on the choice of the functions $b_{\nu n}(p,z)$. In general form, it can be written as[25]

$$\Delta_3B^L(p,k'p';z)=-im4\pi^2t(k',k';z_2-3p'^2/4m)\times\left\{k'B^L(p,k'p';z_1)+\frac{1}{p'}\int dp_1^2B^L(p,\varkappa_1p_1;z_1)\times P_L\left(\frac{mz-p_1^2-p'^2}{p'p_1}\right)\theta\left[1-\frac{|mz-p'^2-p_1^2|}{p'p_1}\right]\right. \tag{82}$$

As one of the possible ways of constructing phenomenological three-particle amplitudes satisfying all the unitarity conditions, we can put forward the following. Choose $b_{\nu n}^L(p,z)$ in the form

$$b_{\nu n}^L(p,z)=a_\nu(k)\,c_n(p,z). \tag{83}$$

Here $a_\nu(k)\equiv a_\nu(k,\ k^2/m)$. For this parametrization, the indices ν and n separate, and the problem greatly simplifies. In addition, for simplicity we restrict ourselves here to a single eigenvalue $n=1$, and (83) is then replaced by

$$b_\nu^L(p,z)=a_\nu(k)\,c(p,z). \tag{84}$$

For the eigenvalue $\nu=\nu_0$ corresponding to the deuteron pole we have $k=i\alpha$, the function $a_{\nu_0}(i\alpha)$ is a number, and one can therefore assume that $b_{\nu_0}^L(p_0,z)=\sqrt{\mu'_{\nu_0}(-\epsilon)}\,\varphi(\alpha)c(p_0,z)$, where $\varphi(\alpha)$ is the deuteron wave function and p_0 is determined by (81). Then from the definition of the three-particle amplitudes (68) and (69) we obtain the representations

$$A_L(p_0,z)=\frac{\varphi^2(\alpha)}{4\pi}\frac{[c(p_0,z)]^2}{1-\gamma(z)}; \tag{85}$$

$$B_L(p_0,kp;z)=t(k)\,\varphi(\alpha)\frac{c(p_0,z)\,c(p,z)}{\sqrt{4\pi}\,[1-\gamma(z)]}, \tag{86}$$

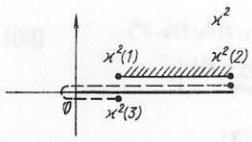

FIG. 35.

where the expansion (45) of the t matrix has been used to derive (86).

In this approximation, the unitarity condition (79) is reduced to an inhomogeneous Hilbert problem and it establishes a direct connection between the eigenvalue $\gamma(z)$ and the choice of the function $c(p,z)$ [17]:

$$1-\gamma(z)=\frac{1}{Q(z)}\left\{\frac{m}{2}\int\limits_{-\varepsilon}^{\infty}\frac{M_{11}(z')\,dz'}{z'-z}+P(z)\right\}. \tag{87}$$

Here, $P(z)$ is an arbitrary function that does not have singularities on the same contour as $\gamma(z)$; M_{11} is determined by Eq. (80), in which we must retain only one eigenvalue and use the parametrization (84); $Q(z)$ is the function defined by

$$c(p,\ x+i\delta)=Q(x)\,c(p,\ x-i\delta). \tag{88}$$

The unitarity condition (87) in principle allows the choice of $c(p,z)$ as a constant, although the additional condition (82) on the FSI cut excludes this possibility since it imposes definite restrictions on the choice of $c(p,z)$; namely, it follows from (82) that

$$\Delta_3 c(p,\ z)=-\frac{im4\pi^2}{p}\int dp_1^2\,t(\varkappa_1,\ \varkappa_1;\ z_1-3p_1^2/m)\,c(p_1,\ z_1)\times P_L\left(\frac{mz-p^2-p_1^2}{pp_1}\right)\theta\left[1-\frac{|mz-p_1^2-p^2|}{pp_1}\right]. \tag{89}$$

Having chosen functions $c(p,z)$ and $\gamma(z)$ which satisfy the conditions (80), (87), and (89), we have thus constructed three-particle amplitudes with all cuts except the dynamical one. In the next section, we shall consider in detail the unitarity conditions on the FSI cut. It is important that one can find solutions for which $c(p,z)$ and accordingly $b(p,z)$ do not have a discontinuity across the cuts Δ_4 and Δ_5, so that the connection between $\gamma(z)$ and $c(p,z)$ remains as in (87) and (80).

5. FINAL-STATE INTERACTION

We begin by considering the unitarity conditions for the final-state interaction. If we restrict ourselves to a single partial wave for the interacting pair ($l=0$), we can always represent B_L in the form

$$B_L(p,\ k'p';\ z)=t(k',\ k';\ z-3p'^2/4m)\,c_L(p,\ k',\ p';\ z). \tag{90}$$

Substituting this expression into the unitarity condition (82), we obtain for c_L exactly the same expression for the discontinuity Δ_3 as in (89) for $c(p',z)$. Since p is unaffected by the unitarity conditions, and k' and p' are related by the law of energy conservation, we can without loss of generality consider Eq. (89).

Note that the representation (90) already separates out explicitly the Migdal-Watson effect, which is described by the first factor. The second factor also contains a dependence on k', which distorts the Migdal-Watson effect. Below, we shall obtain in explicit form this dependence, which physically described the influence of the third particle on the interaction of the pair. The second reason why the Migdal-Watson effect is distorted for identical particles is more trivial and arises because of the symmetrization of the amplitude B_L in the experimentally observed cross section in accordance with Eq. (21).

It is convenient to consider the discontinuity Δ_3, introducing the variables $\varkappa^2\equiv k'^2$ and z instead of p' and z. Then the FSI cut begins at $\varkappa^2=0$ and does not depend on z. Note that in our treatment p' has always been a real number. Therefore, $\varkappa^2$ and z have the same imaginary correction, and the expression for the FSI discontinuity can be rewritten in the form

$$c_L(\varkappa_+^2,\ z_+)-c_L(\varkappa_-^2,\ z_-)=\frac{2}{\sqrt{3}}\cdot\frac{\lambda}{\sqrt{mz-\varkappa^2}}\int\limits_{(\varkappa-\sqrt{3(mz-\varkappa^2)})^2/4}^{(\varkappa+\sqrt{3(mz-\varkappa^2)})^2/4}\frac{d\varkappa_1^2}{\varkappa_1}\left[\exp\left[2i\delta(\varkappa_1)\right]-1\right]\times P_L\left(\frac{\varkappa_1^2+\varkappa^2-5mz/4}{\sqrt{(mz-\varkappa^2)(mz-\varkappa_1^2)}}\right)c_L(\varkappa_+^2,\ z_+). \tag{91}$$

Here we have introduced the parameter $\lambda=1$ for three identical particles, and $\lambda=-1/2$ for the quartet state of three nucleons.

Note that the discontinuity on the left in (91) is not an analytic function of $\varkappa^2$ (in the sense of the difference of the values of an analytic function above and below the cut), since the energy argument z is different in the first and second terms on the left. At the same time, it is $c_L(\varkappa_+^2,z_+)$ that determines the physical value of the amplitude in the experimental cross section. Instead of the discontinuity (91), it is convenient to consider a different discontinuity, only with respect to the variable $\varkappa^2$ for fixed z, and introduce the variable $\varkappa$. Then Eq. (91) is replaced by

$$c_L(\varkappa,\ z_+)-c_L(-\varkappa,\ z_+)=\frac{4}{\sqrt{3}}\cdot\frac{\lambda}{\sqrt{mz-\varkappa^2}}\int\limits_{[\sqrt{3(mz-\varkappa^2)}-\varkappa]/2}^{[\sqrt{3(mz-\varkappa^2)}+\varkappa]/2}d\varkappa_1\left[\exp\left[2i\delta_0(\varkappa_1)\right]-1\right]\times P_L\left(\frac{\varkappa_1^2+\varkappa^2-5mz/4}{\sqrt{(mz-\varkappa^2)(mz-\varkappa_1^2)}}\right)c_L(\varkappa_1,\ z_+). \tag{92}$$

A difference between the right-hand sides of (91) and (92) arises for $\varkappa^2\geq 3mz/4$, when the lower limit in (92) becomes negative, which in the variable $\varkappa^2$ would mean the position of the contour of integration shown in Fig. 35 by the dashed line. The contour of integration in Eq. (91) is indicated in the same figure by the dashed line. Thus, the discontinuities in Eqs. (91) and (92) indicate the different ways of circumventing the singularity, whose position depends on both $\varkappa^2$ and z. The origin of this singularity and its position can be found from Fig. 36, on which we have shown one of the graphs corresponding to Eqs. (91) and (92). The dashed curve corresponds to replacement of the corresponding propagator by a δ function. The graph in Fig. 36 has a triangular anomalous singularity, which arises for $\varkappa^2\geq 3mz/4$,

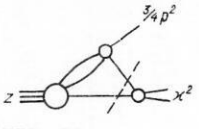

FIG. 36.

$z > 0$. It is important that the triangular anomalous singularities arise only when $\operatorname{Im}\varkappa^2 \cdot \operatorname{Im} z < 0$ [43,44]; therefore, the functions $c_L(\varkappa_+^2, z_+)$ and $c_L(\varkappa_-^2, z_-)$ do not have them, while $c_L(-\varkappa, z_+) \equiv c_L(\varkappa_-^2, z_+)$ does. Accordingly, the solution $c_L(-\varkappa, z_+)$ becomes infinite as $(mz - \varkappa^2)^{-1/2}$ in the limit $\varkappa \to -\sqrt{mz}$, but this must not perturb us, since we are interested in only the final product—the physical amplitude $c_L(\varkappa_+^2, z_+)$, which does not have these singularities.

Equation (92) is a homogeneous integral equation for the function $c_L(\varkappa, z)$, which can be solved explicitly in some of the most interesting cases. The amplitude of two-particle scattering in (92) can be expressed at low energies in the form

$$f_0(\varkappa) = \{\exp[2i\delta_0(\varkappa)] - 1\}/(2i\varkappa) \approx 1/(\alpha - i\varkappa), \tag{93}$$

in which $\alpha = -1/a$, where a is the scattering length. The most characteristic and interesting features of the final-state interaction arise when the scattering length is long, i.e., $\alpha r_0 \ll 1$, where r_0 is the interaction range, so that the form of the amplitude (93) holds in the fairly wide range $\varkappa r_0 \lesssim 1$. When (93) is substituted into Eq. (92), two limiting cases arise. Since the effective values are $\varkappa \sim \sqrt{mz}$ [as can be seen from the limits of integration in (92)], these cases are: 1) $\sqrt{mz} \gg |\alpha|$; 2) $\sqrt{mz} \ll |\alpha|$. Let us consider first case 1) and ignore α in (93) compared with $i\varkappa$. Then, introducing the notation

$$x = \varkappa/\sqrt{mz};\ \psi(x, z) = \sqrt{mz - \varkappa^2}\, c_0(\varkappa, z), \tag{94}$$

we obtain the following equation for ψ if for simplicity we set $L = 0$:

$$\psi(x, z) - \psi(-x, z) = -\frac{8}{\sqrt{3}}\lambda \int_{[\sqrt{3(1-x^2)}-x]/2}^{[\sqrt{3(1-x^2)}+x]/2} dx_1 \frac{\psi(x_1, z)}{\sqrt{1-x_1^2}}. \tag{95}$$

We see a solution of (95) in the form

$$\psi(x, z) = \exp(b \arcsin x) - D\exp(-b \arcsin x). \tag{96}$$

From the condition that $c(\varkappa, z)$ be finite for $\varkappa = \sqrt{mz}$ we obtain $D = \exp(b\pi)$, and then substituting the solution (96) into Eq. (95) we obtain a condition on the parameter b:

$$\operatorname{ch} b\pi/2 = (8\lambda/\sqrt{3}b)\operatorname{sh} b\pi/6. \tag{97}$$

The condition (97) coincides with the corresponding condition for the roots in Ref. 45. This is not surprising since Eq. (95) can be obtained from the Skornyakov—Ter-Martirosyan equation (46) which was written down in Ref. 45 in the approximation $\sqrt{mz} \gg \alpha$. Indeed, it is obtained by taking the discontinuity with respect to the variable p_1 in Eq. (1) of Ref. 45. Therefore, the solution (96) also corresponds to the solution of the Skornyakov—Ter-Martirosyan equation in the first limiting case $\sqrt{mz} \gg \alpha$ investigated in Refs. 47 and 48.

Note that the equation for the discontinuity (95) determines only the dependence on the variable $\varkappa$ (or rather, $x = \varkappa/\sqrt{mz}$) and in no way determines the dependence on z or the initial momentum p in the breakup amplitude $B_L(p, k'p'; z)$. This is perfectly natural, since the unitarity conditions do not uniquely determine the amplitude, in contrast to the dynamical equations, and, therefore, to find the amplitude one must in addition specify the analytic properties at the nearest singularities, as we discussed above.

The case $L \neq 0$ can be studied in the same way as in Ref. 45, and the solution again written down explicitly. Here we shall not dwell on this question.

Note that Eq. (97) has a root $b \sim 1$ and therefore in the function ψ the variable $\varkappa$ varies over distances of order $\sqrt{mz} \gg |\alpha|$, whereas the first term in (90)—the "pure" Migdal-Watson effect—varies appreciably over distances $\varkappa \sim |\alpha|$. Therefore, subject to the condition (1), $\sqrt{mz} \gg \alpha$, exact allowance for FSI hardly distorts the simple Migdal-Watson expression. In addition, the distortions resulting from symmetrization for identical particles are also small under this condition.

We now turn to the case of low energies, when the condition (2) holds: $\sqrt{mz} \ll \alpha$. Instead of (95) we now have

$$\psi(x, z) - \psi(-x, z) = \frac{8i\lambda}{\sqrt{3}} \cdot \frac{\sqrt{mz}}{\alpha} \int_{[\sqrt{3(1-x^2)}-x]/2}^{[\sqrt{3(1-x^2)}+x]/2} \frac{x_1\, dx_1}{\sqrt{1-x_1^2}} \psi(x_1, z). \tag{98}$$

Because of the small factor in front of the integral in (98), this equation can be solved by iteration:

$$\psi(x, z) = \psi_0(x, z) + \frac{\sqrt{mz}}{\alpha}\psi_1(x, z) + \ldots \tag{99}$$

For small z, the function ψ, which depends analytically on $\varkappa$ and z in the neighborhood of $\varkappa = 0$ and $z = 0$, can be expanded in a series with respect to these arguments and one need retain only the constant term in ψ_0. Then (98) determines ψ_1 in terms of ψ_0 to terms of order $\varkappa^2/\alpha^2$:

$$\psi(x, z) = \psi_0(0, 0)\left(1 + 8i\lambda \frac{\sqrt{mz}}{\alpha} x\right) + \ldots \tag{100}$$

This procedure is essentially the simplest variant of the expansion used in Refs. 49 and 50. The practical aim of such an expansion is to recover from experimental data α, which is proportional to the scattering length: for example, in the case of $\pi N \to \pi\pi N$ reactions or $K \to 3\pi$ decays, to extract the $\pi\pi$ scattering length. Equation (98) in conjunction with (90) shows that this is in principle possible since the unknown ψ_0 enters as a common factor. However, as was noted in Refs. 49 and 50, for identical particles the modulus of the square of the expression (100), which occurs in the cross section, contains $\varkappa^2/\alpha^2$ and not $\varkappa/\alpha$. Terms of the same form arise in the cross section and the decay probability from the expansion of $\psi(\varkappa, z)$ in powers of z since $z \sim \varkappa_{12}^2 + \varkappa_{13}^2 + \varkappa_{23}^2$, but the coefficient of z is unknown. Therefore, in the case of identical particles this procedure for finding the scattering lengths does not work, although for nonidentical particles term linear in $\varkappa/\alpha$ can arise in the cross section.[49] In Refs. 49 and 50, besides the fairly trivial case $\sqrt{mz}/|\alpha| \ll 1$ and the equivalent case $\sqrt{mz}/|\alpha_{ik}| \ll 1$ for three nonidentical particles, an investigation was also made of the case when this condition is satisfied for two pairs of particles but not satisfied for one of the pairs: $\sqrt{mz}/\alpha_{12} \gtrsim 1$. In the amplitude, only terms of first order in $\sqrt{mz}/|\alpha_{ik}| \sim \sqrt{mz}r_0$ and any order in the ratio $\sqrt{mz}/|\alpha_{12}|$ were retained. The same results

can be readily reproduced in the present formalism. Instead of Eq. (91) for nonidentical particles we have a system of three equations for the amplitudes $C_L^{(ik)}$ containing $t^{(ik)}$ in the kernels. Therefore, the solution reduces to iteration of this system with retention of terms proportional to $t^{(23)} \sim r_0$ and $t^{(13)} \sim r_0$. However, Eq. (91) in principle gives one the possibility of obtaining a solution in the general case as well, when all three pairs are in resonance.

6. THREE-PARTICLE RESONANCES

We consider a system of three particles interacting in such a way that at least two of the three pairs form a two-particle resonance. For identical particles, which we mainly consider here, a resonance must be present in each of the three pairs. The question arises of whether in such a system a three-particle resonance (or a bound state) arises and what will be the analytic structure of the three-particle amplitude. We shall show in what follows that, using the unitarity conditions derived in Sec. 3, one can answer this question fairly fully and determine the conditions under which a resonance or some other structure arises in the three-particle system.

We shall proceed from the unitarity conditions (9)—(14) for the amplitude w and define purely formally the amplitude C_L, which in what follows we shall call the amplitude of the resonance particle:

$$w(k\mathbf{p};\ k'\mathbf{p}';\ z) = \sum_L (2L+1)\, P_L(\cos\theta_{pp'})\, t(k)\, C_L(p, p', z)\, t(k'). \tag{101}$$

From (9)—(14) for the amplitude C_L one can then readily obtain unitarity conditions which have the same structure but do not contain the terms Δ_{2d} or Δ_{3d}. We also omit the term Δ_5, assuming that there are no bound states in the two-particle system. As we have already mentioned, Δ_2 and Δ_3 are related physically to the FSI effect, and therefore mathematically they are exactly equal to the discontinuities of C_L with respect to the variables p and p', or rather the variables $\sigma = k^2/m$ and $\sigma' = k'^2/m$ (the latter are more convenient, since the branch points with respect to σ and σ' do not depend on z). Thus, for the amplitude $C_L(\sigma, \sigma'; z)$ we obtain the following expression for the discontinuity with respect to the variable z:

$$\Delta_z C_L(\sigma, \sigma', z) = J_1 + J_4 + J_5, \tag{102}$$

where

$$J_1 = -\frac{2\pi m i}{pp'} P_L[x(p, p')]\, \theta[1 - |x(p, p')|]; \tag{103}$$

$$J_4 = -\frac{32}{3} i m^2 \pi^3 \int d\sigma_1 k_1(\sigma_1)\, |t(k_1)|^2\, C_L(\sigma, \sigma_1 + i\delta, z + i\delta) \times C_L(\sigma_1 - i\delta, \sigma', z - i\delta); \tag{104}$$

$$J_5 = -\frac{128}{9} i m^3 \pi^3 \int\int d\sigma_1\, d\sigma_2 C_L(\sigma, \sigma_1 + i\delta, z + i\delta) \times C_L(\sigma_2 - i\delta, \sigma', z - i\delta)\, t(k_1)\, t^*(k_2') \times P_L[x(p_1, p_2)]\, \theta[1 - |x(p_1, p_2)|]. \tag{105}$$

Here we have everywhere taken into account the energy conservation law

$$z = k^2/m + 3p^2/(4m) = \sigma + 3p^2/(4m) = k'^2/m + 3p'^2/(4m) = \sigma' + 3p'^2/(4m)$$

and introduced the notation

$$x(p, q) = (mz - p^2 - q^2)/(pq). \tag{106}$$

In our statement of the problem, the two-particle t matrix is given by the Breit-Wigner expression:

$$t(k) = \Gamma/[4\pi^2 mk\,(k^2/m - \epsilon + i\Gamma/2)], \tag{107}$$

where Γ is the total width; ϵ is the excitation energy of the resonance. Then one can show that the term J_5 is small compared with J_4, namely, $J_5/J_4 \lesssim \Gamma/z$.

In the situation of interest to us, the three-particle resonance must decay into a two-particle resonance and a third particle—states which are present in J_4—and not into three uncorrelated particles, which make the main contribution to J_5. Physically, this justifies the neglect of J_5 compared with J_4.

Note also two important factors that are usually ignored in the literature (see Refs. 51—54 and the references cited there). First, $C_L(\sigma, \sigma', z)$ has singularities and corresponding discontinuities with respect to σ and σ', and one must distinguish the sides of the cut in the σ and σ' planes on which the value of the function is taken. Second, it is only for the function $C_L(\sigma - i\delta, \sigma' + i\delta; z)$ that the unitarity conditions (104) contain the same functions on the right-hand side of the unitarity conditions as on the left, i.e., form a closed system of equations. In (104) one can, to within terms of order Γ^2/z^2, extract the function C_L at the point of the pole $\sigma_1 = \epsilon$. Then, integrating with the remaining part of the integrand, we obtain [we set also $\sigma = \sigma' = \epsilon$ and denote $C_L(\epsilon - i\delta,\ \epsilon + i\delta.\ z) \equiv C_L(z)$]

$$\left.\begin{aligned} &\Delta_z C_L(z) = \frac{2\pi m i}{p_R^3} P_L[x(p_R.\ p_R)] \times \theta[1 - |x(p_R.\ p_R)|] - \\ &-\frac{4}{3} \cdot \frac{i\Gamma p_R}{\sqrt{m\epsilon}}\, \theta(z - \epsilon)\, C_L(z + i\delta)\, C_L(z - i\delta);\ p_R^3 = 4m(z - \epsilon)/3. \end{aligned}\right\} \tag{108}$$

Equation (108) is very similar to the two-particle unitarity condition, and the first term acquires the meaning of the dynamical (usually the left-hand) cut. It is convenient to go over to the dimensionless variable $y = (z - \epsilon)/\epsilon$ and by an obvious substitution replace C_L by a new function $M(y)$, for which the unitarity condition takes the form

$$\Delta M(y) = 2i\xi(y)\, \theta(y - y_1)\, \theta(y_2 - y) + 2i\theta(y) \sqrt{y}\, M(y - i\delta)\, M(y + i\delta). \tag{109}$$

Equation (109) can be derived similarly for relativistic particles; we give the values of all the parameters in (109) for a relativistic case when the three spinless particles have masses μ, μ, m; the mass of the two-particle resonance in the $\mu + m$ system is $\mu + m + \epsilon$, and the square of the total energy of the three particles is S, as is shown in Fig. 37. In this case

$$\left.\begin{aligned} &y = [S - (m + 2\mu + \epsilon)^2]/[2\epsilon(m + 2\mu + \epsilon)]; \\ &\xi(y) = \pi\Gamma\zeta P_L(u_0)/4\epsilon y; \end{aligned}\right\} \tag{110}$$

where

$$\zeta = \frac{(m + \mu - \epsilon)^3\, [2\mu(m + \mu + \epsilon) + \epsilon(m + 2\mu + \epsilon)\, y]^{-1/2}}{\sqrt{(2m + 2\mu + \epsilon)(m + \epsilon/2)(\mu + \epsilon/2)(2\mu + m + \epsilon)}}; \tag{111}$$

$$y_1 = \frac{2m + \epsilon}{2(m + 2\mu + \epsilon)} \leqslant 1;\quad y_2 = \frac{(m + 2\mu + \epsilon)(2m + \epsilon)}{2m^2} \geqslant 1. \tag{112}$$

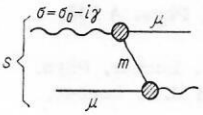

FIG. 37.

The value of u_0 is determined by the energy y and is the cosine of the scattering angle in the graph in Fig. 37 at the point of the pole. The parameter ξ depends on the masses and the energy and is everywhere greater than unity.

Equation (109) can be solved if, as in the ordinary N/D method, we represent the amplitude in the form

$$M(y) = N(y)/D(y). \tag{113}$$

and require that the discontinuity $\xi(y)$ be given by the function $N(y)$. However, in contrast to the ordinary procedure[33] the singularities of $D(y)$ and $N(y)$ are here not separated by any interval. From (109) and (113) we obtain

$$N(y) = \frac{1}{\pi}\int_{y_1}^{y_2}\frac{dy'}{y'-y}\xi(y')\,D(y'_-); \tag{114}$$

$$D(y) = 1 - \frac{y}{\pi}\int_0^{\infty}\frac{dy'}{y'-y}\cdot\frac{N(y'_-)}{\sqrt{y'}}, \tag{115}$$

where the subscript — means that the value of the function is taken on the lower edge of the cut. Substituting (114) into (115), one can obtain an exact solution in the form

$$D(y) = \exp\left\{-\frac{\sqrt{y}}{2\pi i}\int_{x_1}^{x_2}\frac{dx'}{x'(x'+\sqrt{y})}\ln g(x')\right\}, \tag{116}$$

where $x = \sqrt{y}$;

$$g(x) = 1 - 4x\xi(x^2); \tag{117}$$

for $L=1$, the solution (116) must be multiplied by

$$P(x) = \left(1 + \frac{\sqrt{y}}{2\pi i}\int_{x_1}^{x_2}\frac{dx'}{x'^2}\ln g(x')\right). \tag{118}$$

Note that this solution corresponds to summation of the ladder graphs shown in Fig. 38. Since we have hitherto ignored the left-hand cuts, our solution is the exact value of the sum of graphs in the limiting case $\epsilon \ll m$, μ, when the left-hand cuts go to $-\infty$. In the general case, allowance for the left-hand cuts does not change the analytic properties of the solution obtained.

The main properties of the solution are as follows:

1) on the physical sheet, i.e., where $\sqrt{y} > 0$, there are no Peierls singularities in the denominator of the resonance-particle amplitude. This conclusion contradicts the results of Refs. 51—54. One can show that the error of these papers results from the incorrect relative position of the dynamical and the unitary cut;

2) for $L=0$ on the physical sheet there are no poles corresponding to three-particle resonances or bound states of the resonance and a particle. However, in the case of sufficiently strong attraction ($\xi > 0$), when $g(x) < 0$ on the interval $[x_3, x_4]$, a square-root branch point

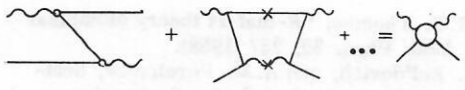

FIG. 38.

arises in the amplitude $M(y)$, leading to a peak; namely,

$$|M(y)|^2 = \left|\sqrt{\frac{x_3(x_4+\sqrt{y})}{x_4(x_3+\sqrt{y})}}\right|^{\pm 2}; \tag{119}$$

3) for $L=1$, besides this square-root singularity, poles can arise because of the zeros of the factor (118). In the case of attraction, $\xi > 0$, there arises a pole of bound-state type ($y < 0$), when $g(x)$ is everywhere positive. In the case of even stronger attraction, when $g(x)$ becomes zero, the pole goes into the complex plane and takes on an additional width.

Let us consider applications of our formalism. They are possible in molecular, atomic, and nuclear physics and also in the physics of elementary particles. Let us discuss two examples. If in a nuclear system consisting of three particles (three clusters or a core plus two nucleons) a resonance arises in the two-particle systems, then for sufficiently large $\xi \sim \Gamma\zeta/\epsilon$ there arises a three-particle resonance or singularity of the type (119). The calculations show that the 2^+ level of ^{8}Be (two α particles) can produce a system of three resonances $J^P = 1^-$, 2^-, 3^- in the system of three α particles (nucleus of ^{12}C). However, the most favorable case is that of a core nucleus plus two nucleons, since ζ in (111), and therefore ξ as well, is proportional to the mass ratio of the core nucleus and the nucleon. This mechanism can lead to the appearance of levels of the nucleus of a quite singular nature.

In the field of elementary particles, we have investigated the ΔN system with different quantum numbers. It was found that in the states J^P, $T = 1^+, 2$ and $2^+, 1$ there arises a singularity of the type (119), and $x_4/x_4 \approx 3$, so that the peak (or dip; here two solutions are possible) exceeds the background by a factor of three and develops over a width $\Delta E \sim 150$ MeV near the threshold of ΔN formation. For $L=1$, a resonance arises in the ΔN system with mass determined by Eq. (118).

It has the quantum numbers $J^P = 0^-$, $T=2$ and an energy approximately 350 MeV higher than twice the nucleon mass; its width is $\gtrsim 70$ MeV. The ΔN system has previously been considered by other methods.[55,56] Gale and Duck[55] used Faddeev's equation and found in the relativistic kinematics a 0^- resonance with $T=2$ at an energy exactly agreeing with our calculation. They also noted attraction in the 1^+ states with $T=2$ and 2^+ states with $T=1$, in which the root branch points arise in our case. Bound states do not occur in their numerical calculations, in agreement with our conclusions. The above examples demonstrate the simplicity of the calculations and the efficiency of the method presented in this section.

[1]A. M. Lane and R. G. Thomas, "*R*-matrix theory of nuclear reactions," Rev. Mod. Phys. **30**, 257 (1958).
[2]A. I. Baz', Ya. B. Zel'dovich, and A. M. Perelomov, Scattering, Reactions and Decay in Nonrelativistic Quantum Mechanics, Jerusalem (1969).
[3]L. D. Blokhintsev, É. I. Dolinskiĭ, and V. S. Popov, Zh. Éksp. Teor. Fiz. **42**, 1636 (1962); **43**, 1914 (1962) [Sov. Phys.-JETP, **15**, 1136 (1962); **16**, 1350 (1962)].
[4]M. L. Goldberger and K. M. Watson, Collision Theory, New York (1964).
[5]L. D. Faddeev, Zh. Éksp. Teor. Fiz. **39**, 1459 (1960); [Sov. Phys.-JETP, **12**, 1014 (1961)]; Tr. Matem. In-ta **69**, 1 (1963).
[6]I. S. Shapiro, Teoriya Pryamykh Yadernykh Reaktsiĭ, Moscow, Gosatomizdat (1963). [Theory of Direct Nuclear Reactions].
[7]I. H. Sloan, Phys. Rev. **165**, 1587 (1968).
[8]G. F. Chew, The Analytic *S*-Matrix, New York-Amsterdam (1966).
[9]See Ref. 4, Ch. 11.
[10]W. R. Frazer and J. R. Fulco, Phys. Rev. Lett. **2**, 365 (1959).
[11]A. G. Baryshnikov *et al.*, ZhÉTF Pis'ma Red. **16**, 414 (1972) [JETP Letters **16**, 294 (1972)].
[12]R. T. Cahill and I. H. Sloan, Nucl. Phys. A **194**, 589 (1972).
[13]R. T. Cahill, Nucl. Phys. A **194**, 599 (1972).
[14]R. Tandy, R. Cahill, and I. E. McCarthy, Phys. Lett. B **41**, 241 (1972).
[15]K. L. Kowalski, Phys. Rev. D **5**, 395 (1972).
[16]A. M. Badalyan and Yu. A. Simonov, Teoriya Dvukh- i Trekhchastichnykh Rezonansov. Lektsiya Letneĭ Shkoly MIFI (1973) [Theory of Two- and Three-Particle Resonances. Summer School Lectures, Moscow Engineering Physics Institute].
[17]Yu. A. Simonov and A. M. Badalyan, Preprint ITÉP-89 (1973).
[18]C. Lovelace, Phys. Rev. B **135**, 1225 (1964). E. Harms and J. S. Levinger, Phys. Lett. B **30**, 449 (1969).
[19]I. M. Narodetsky, E. S. Galpern, and V. N. Lyakhovitsky, Phys. Lett. B **46**, 51 (1973).
[20]V. M. Kolybasov, Problemy Sovremennoĭ Yadernoĭ Fiziki, Nauka, Moscow (1971), p. 391 [Problems of Modern Nuclear Physics].
[21]J. D. Seagrave, in: Three-Body Problem (Eds. J. S. C. McKee and P. M. Rolph), Amsterdam-London (1970), p. 41.
[22]A. P. Rudik and Yu. A. Simonov, Zh. Éksp. Teor. Fiz. **45**, 1016 (1963) [Sov. Phys.-JETP **18**, 703 (1960)].
[23]I. Šlaus, in: Three-Body Problem (Eds. J. S. C. McKee and P. M. Rolph), Amsterdam-London (1970), p. 337.
[24]G. F. Chew and S. Mandelstam, Phys. Rev. **119**, 467 (1960).
[25]A. M. Badalyan and Yu. A. Simonov, Preprint ITÉP-61 (1973).
[26]R. Blankenbecler, M. Goldberger, and F. Halpern, Nucl. Phys. **12**, 629 (1959).
[27]M. P. Locher, Nucl. Phys. B **23**, 116 (1970).
[28]R. E. Cutkosky and B. B. Deo, Phys. Rev. **174**, 1859 (1968).
[29]L. S. Kisslinger, Phys. Rev. Lett. **29**, 505 (1972).
[30]T. E. O. Ericson and M. P. Lochner, Nucl. Phys. A **148**, 1 (1970).
[31]T. E. O. Erickson, J. Formànek, and M. P. Locher, Phys. Lett. B **26**, 91 (1967); T. E. O. Ericson and M. P. Locher, Phys. Lett. B **27**, 576 (1968).
[32]L. S. Kisslinger, Preprint MIT (1973).
[33]G. Barton and A. C. Phillips, Nucl. Phys. A **132**, 97 (1969); Y. Avishai, W. Ebenhöh, and A. S. Rinat-Reiner, Ann. Phys. **55**, 341 (1969); R. H. Bower, Ann. Phys. **73**, 372 (1972).
[34]T. Sasakawa, Nucl. Phys. A **186**, 417 (1972).
[35]T. Sasakawa, Paper presented to the Los-Angeles Conference (1972).
[36]S. Weinberg, Phys. Rev. **131**, 440 (1963).
[37]S. I. Manaenkov, Teor. Mat. Fiz. **12**, 397 (1972).
[38]I. M. Narodetskii, Yad. Fiz. **9**, 1086 (1969) [Sov. J. Nucl. Phys. **9**, 636 (1969)].
[39]M. G. Fuda, Phys. Rev. **174**, 1134 (1968); I. M. Narodetskiĭ, Yad. Fiz. **12**, 61 (1970) [Sov. J. Nucl. Phys. **12**, 33 (1970)].
[40]A. G. Sitenko and V. F. Kharchenko, Usp. Fiz. Nauk **103**, 469 (1971) [Sov. Phys.-Uspekhi. **14**, 125 (1971)].
[41]A. M. Badalyan and Yu. A. Simonov, Preprint ITÉP-966 (1972).
[42]E. S. Gal'pern, V. N. Lyakhovitskiĭ, and I. M. Narodetskiĭ, Preprint [in Russian], ITÉF 927 (1972); Yad. Fiz. **16**, 707 (1972) [Sov. J. Nucl. Phys. **16**, 395 (1973)].
[43]R. Blankenbecler and Y. Nambu, Nuovo Cimento **18**, 595 (1960).
[44]Yu. A. Simonov, Zh. Éksp. Teor. Fiz. **43**, 2262 (1962) [Sov. Phys.-JETP **16**, 1599 (1963)].
[45]N. N. Beloozerov, Yad. Fiz. **2**, 552 (1965) [Sov. J. Nucl. Phys. **2**, 395 (1966)].
[46]G. C. Skornyakov and K. A. Ter-Martirosyan, Zh. Éksp. Teor. Fiz. **31**, 775 (1956) [Sov. Phys.-JETP **4**, 648 (1957)].
[47]G. S. Danilov, Zh. Éksp. Teor. Fiz. **40**, 498 (1961); **43**, 1424 (1962) [Sov. Phys.-JETP **13**, 349 (1962); **16**, 1010 (1963)].
[48]R. A. Minlos and L. D. Faddeev, Zh. Éksp. Teor. Fiz. **41**, 1850 (1961) [Sov. Phys.-JETP **14**, 1315 (1962)].
[49]V. N. Gribov, Zh. Éksp. Teor. Fiz. **38**, 553 (1960); **41**, 1221 (1961) [Sov. Phys.-JETP **11**, 400 (1960); **14**, 871 (1962)].
[50]V. V. Anisovich, A. A. Ansel'm, and V. N. Gribov, Zh. Éksp. Teor. Fiz. **42**, 224 (1962) [Sov. Phys.-JETP **15**, 159 (1962)].
[51]J. R. Aitchison and D. Krúpa, Nucl. Phys. A **182**, 449 (1972).
[52]R. F. Peierls, Phys. Rev. Lett. **6**, 641 (1961).
[53]S. Mandelstam *et al.*, Ann. Phys. **18**, 198 (1962).
[54]D. D. Brayshaw and R. F. Peierls, Phys. Rev. **177**, 2539 (1968).
[55]W. A. Gale and I. M. Duck, Nucl. Phys. B **8**, 109 (1968).
[56]L. A. Kondratyuk and I. S. Shapiro, Yad. Fiz. **12**, 401 (1970) [Sov. J. Nucl. Phys. **12**, 220 (1970)].

Translated by Julian B. Barbour